SLAC-29
UC-28, Particle Accelerators
and High-Voltage Machines
UC-34, Physics
TID-4500 (35th Ed.)

SPECIFICATIONS FOR THE BEAM TRANSPORT SYSTEMS TO END STATIONS A AND B

June 1964

by

H. S. Butler*, S. K. Howry and C. H. Moore

Technical Report
Prepared Under
Contract AT(04-3)-400
for the USAEC
San Francisco Operations Office

*Now with Los Alamos National Laboratory, Los Alamos, New Mexico

Printed in USA. Price $3.00. Available from the Office of Technical Services, Department of Commerce, Washington 25, D.C.

TABLE OF CONTENTS

I. INTRODUCTION

In order to use effectively the electron beam from the Stanford two-mile linear accelerator, an elaborate beam switchyard will be needed. Of primary importance in the switchyard is the beam transport system, a series of magnets which will provide the deflections necessary to allow the various experimental areas to be reasonably well separated from each other both physically and radiologically. Present planning calls for two transport systems--one leading to end station A, an area primarily for electron and positron scattering and photoproduction experiments, the other leading to end station B, an area planned for secondary particle production. In addition to deflecting the beam, each transport system will momentum-analyze the beam before directing it toward the appropriate end station. The two transport systems as presently envisioned are shown schematically in Fig. 1.* Both systems will be serviced by the same pulsed switching magnet.

The beam transport system leading to end station A will be referred to as system A in this report. Similarly, system B refers to the transport system leading to end station B. The two systems will be treated separately, system A being considered first. However, the inherent similarity of the two systems means that qualitative remarks made about system A will be applicable to system B.

The essential optics of these two systems were proposed several years ago by K.L. Brown. System A was studied on a semi-quantitative basis by Penner,[1] who concurred that it would be an acceptable system subject to more precise calculations.

It is the purpose of this report to present the results of a long series of calculations which culminated in a set of specifications for the transport systems shown in Fig. 1. The requirements imposed on the system leading to end station A are given in Section II. The design philosophy of the system is discussed in Section III. Section IV contains

---

*The beam line for a proposed gamma ray beam is also shown on this layout. A discussion of this beam is given in Section IV. The momentum defining slit in each system is indicated with dotted lines. The precise configuration of these slits is not known at present.

Report Nomenclature	ABA Nomenclature
P	PM1, PM2, PM3, PM4, PM5
System A	
Q_1	Q10, Q11
B_1	B10, B11, B12, B13
Q_2	Q12
Slit	SL10
B_2	B14, B15, B16, B17
Q_3	Q13, Q14
Q_4	(not labeled by ABA)
System B	
Q_1	Q30, Q31
B_1	B30, (B31-Phase II), B32
Q_2	Q32
Slit	SL30
B_2	B33, (B34-Phase II), B35
Q_3	Q33, Q34

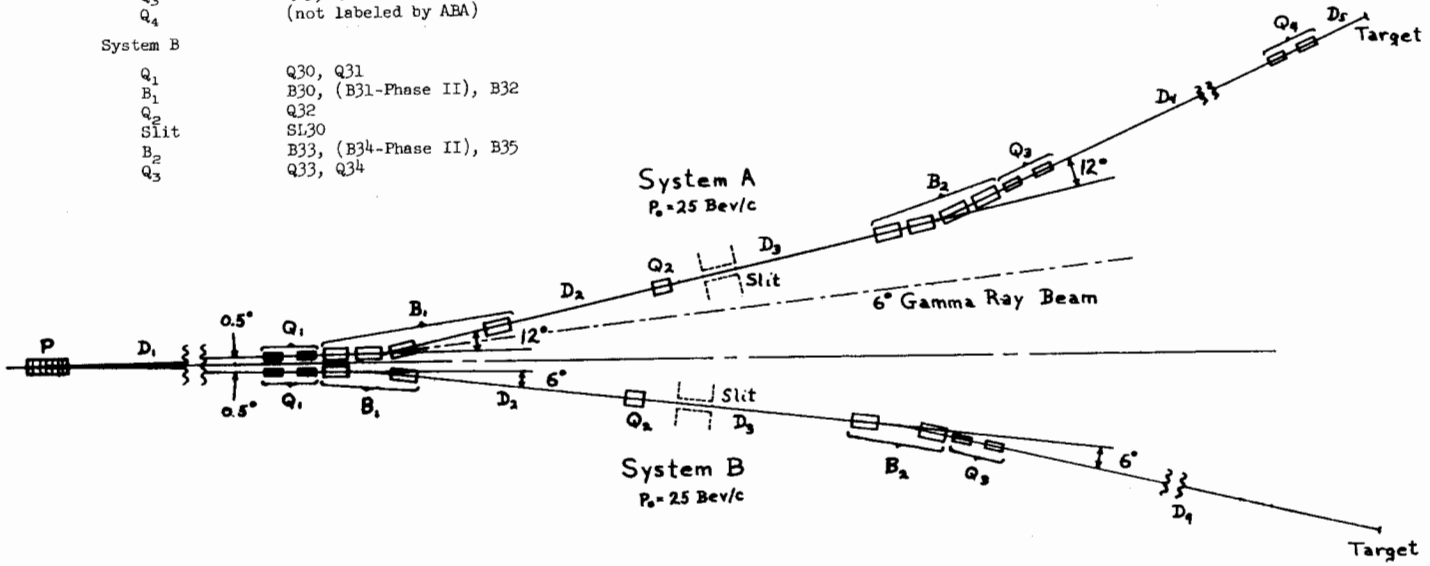

FIGURE 1

the first-order solution to the design problem. Second-order effects are considered in Section V, and alignment tolerances are discussed in Section VI. The requirements for system B are given in Section VII, together with the first-order solution to the system and a discussion of second-order effects and alignment tolerances.

Any description or discussion of the design of a transport system must necessarily be of the "open end" variety; there are always more questions to be answered and new facets of the design to be investigated. This report documents all of the work done on the two systems through February 1964.

The following notation has been adopted in discussing the differential beam coordinates. The quantities x and θ refer to the beam size and divergence, respectively, in the horizontal (radial) plane. The quantities y and φ refer to the vertical plane. The variable z is the differential path length. The quantity $\delta = \Delta p/p$ is the momentum spread in the beam. The transformation equation for the six differential coordinates of an electron is given in Fig. 2.

$$\begin{pmatrix} x \\ \theta \\ y \\ \varphi \\ z \\ \delta \end{pmatrix} = \begin{pmatrix} (x|x_o) & (x|\theta_o) & & & & (x|\delta_o) \\ (\theta|x_o) & (\theta|\theta_o) & & & & (\theta|\delta_o) \\ & & (y|y_o) & (y|\varphi_o) & & \\ & & (\varphi|y_o) & (\varphi|\varphi_o) & & \\ (z|x_o) & (z|\theta_o) & & & 1 & (z|\delta_o) \\ & & & & & 1 \end{pmatrix} \begin{pmatrix} x_o \\ \theta_o \\ y_o \\ \varphi_o \\ z_o \\ \delta_o \end{pmatrix}$$

Figure 2

II. DESIGN CRITERIA FOR SYSTEM A

The following requirements were imposed upon system A either by the properties of the input beam or by the nature of the experiments to be performed utilizing the beam in the end station.

Energy

The design momentum was fixed at 25 GeV/c.

Beam Size

The radius of the beam entering the system was assumed to be 0.3 cm.

Beam Divergence

The angular divergence of 10^{-4} radians was assumed for the input beam.

Momentum Spread

The range of momenta which system A has to pass was fixed at ±1 percent.*

Resolution

The transport system must be capable of resolving ±0.05 percent in momentum at the slit. The mean momentum of the beam should be reproducible to within ±0.02 percent. The momentum spread and mean momentum passed by the system should be independent of the operation of the accelerator and of the performance of the pulsed switching magnet.

Achromaticity

The transport system must be achromatic; that is, after leaving the last bending magnet, the position and divergence of the beam must be independent of the momentum spread. This requires that the elements $(x|\delta_o)$ and $(\theta|\delta_o)$ of the total transformation matrix be identically zero.

Isochronism

In passing through a system of bending magnets, an electron bunch will be spread longitudinally depending on the differential position, divergence, and momentum of the electrons in the bunch. Requiring that the system be achromatic automatically removes the dependence on position and divergence, but still leaves a dependence on the momentum spread of the electrons. After passing through the system the longitudinal extent of the bunch must not exceed ±20° in rf phase (at 2856 Mc/sec) for $\Delta p/p$ = ±1 percent; this is equivalent to a bunch length of ±0.6 cm.

---

*The final design for system A will pass almost ±2 percent, but second-order effects--notably the $(\theta|\theta_o\delta_o)$ and other aberrations associated with δ_o--begin to deteriorate the beam quality above ±1 percent. See Section V.

III. QUALITATIVE DESCRIPTION OF SYSTEM A

Each of the various magnets and drift spaces in system A, as pictured in Fig. 1, serves a specific function. It is the purpose of this section to discuss those various functions and their contributions toward satisfying the design criteria listed in Section II.

A. General Features

The design is characterized by the following basic features. The input beam is assumed to be defined by one means or another at the center of the pulsed magnet, P. The doublet Q_1 forms a double image of the center of the pulsed magnet on the slit, which is assumed to be located at the exit face of the symmetry quadrupole, Q_2. The bending magnet B_1 disperses the beam for momentum resolution at the slit. The symmetry quadrupole has little effect on the beam vertically because of the small vertical size of the beam resulting from the vertical focus at the energy slit. However, in the radial plane the symmetry quadrupole recombines the different momenta, so that after passing through the second set of bending magnets, B_2, the beam will be achromatic. The doublet Q_3 produces a low divergence beam by imaging (approximately) the slit to infinity. The final beam then drifts without appreciable spreading to the end station.

B. Switching Magnet P

The angle of bend of the switching magnet has been fixed at 0.5° for a 25 GeV/c beam. The difficulties in designing a pulsed magnet that will have the necessary stability and reliability characteristics at a reasonable cost and whose operating energy can be programmed on a pulse-to-pulse basis set an upper limit on the angle of bend.

C. Drift Space D_1

After passing through the switching magnet, the deflected beam must drift until it is sufficiently offset from the center line of the straight-ahead beam to allow insertion of the next magnet of the system. A drift of 78.5 meters gives an offset distance of 70 cm (27.5 inches), and this was considered sufficient for the insertion of the next magnets.

This drift space is important for another reason. It fixes the ultimate (zero slit width) resolution of the system. To a first approximation, the minimum $\Delta p/p$ which can be resolved by system A is

$$\left(\frac{\Delta p}{p}\right)_{min} = \frac{\text{beam size}}{\text{offset distance}} = \frac{x_o}{D_1 \times \alpha}$$

where α is the total angle of bend of the first group of bending magnets and x_o is the beam size at the center of the switching magnet. For $\alpha = 12^o$, $x_o = 0.3$ cm and $D_1 = 78.5$ meters,

$$(\Delta p/p)_{min} = 0.018\%$$

D. Quadrupole Doublet Q_1

This doublet images the center of the pulsed magnet onto the slit, which is assumed to be at the exit face of the symmetry quadrupole, Q_2. The gradients of Q_1 are adjusted so that the matrix elements $(x|\theta_o)$ and $(y|\varphi_o)$ of the total transformation matrix between these two points vanish. Adjusting the system in this manner decouples the resolution and momentum-defining qualities of the transport system from any first-order dependence on the performance of the accelerator or the pulsed switching magnet. The image size, and hence the resolution at the slit, is only a function of the size of the beam at the center of the switching magnet, and this can be defined by a collimator at the entrance face of P. If any beam at all gets through the transport system, it will have a mean momentum and a spread in momentum that are within the required tolerances. Of course, the finite length of the real slit will disturb this ideal situation in a manner not yet analyzed.

The first quadrupole of the doublet is made to focus vertically in order to increase the resolution. With this polarity the horizontal principal planes of the doublet are several meters downstream from the actual magnet. This means that D_1 is effectively longer than 78.5 meters and the ultimate resolution is enhanced. Also, the larger vertical image at the slit resulting from the (- +) arrangement reduces the power density

the slit has to tolerate by a factor of two in the vertical plane.

E. Bending Magnet B_1

This magnet serves a dual purpose: it deflects the beam so that the end stations can be physically separated, and it disperses the beam for momentum analysis. The angle of bend was fixed at 12° as a rather loose compromise between two conflicting requirements. The first was economic--the larger the angle of bend, the shorter would be the tunnel housing the system and leading to the end station. There is a net saving between the cost of one degree of bend and the cost of the length of tunnel saved. The second constraint was optical--the greater the angle of bend, the greater the deterioration of the beam isochronism.* For a momentum band pass of ±1 percent, a $12^\circ + 12^\circ$ bend increases the bunch spread by 15° in rf phase. This increase, when combined with the initial bunch length, makes the total bunch length near the limiting value of 20°.

Because of the length of magnet needed to bend 12° (12 meters), the angle of bend will be obtained from four 3-meter magnets each bending 3°. The fourth of these magnets has been moved nine meters downstream to allow clearance for the 6° gamma beam. This modification is discussed in Section IV.

F. Drift Space D_2

After traversing the bending magnet, the beam is dispersed. The distance D_2 is fixed by the momentum spread desired through a fixed slit width. The distance chosen allows a momentum interval of 0.1 percent through a 1/4-inch slit.

G. Symmetry Quadrupole Q_2

This magnet is necessitated by the requirement for an achromatic system; that is, it functions as a field lens to recombine the momenta that were spread out by B_1, in order to bring the beam down to an

---

*There is no fundamental optical limitation to achieving isochronism. If a slight bend in the opposite sense to B_1 were inserted at the center of the system, either by a bending magnet or by a displacement of the symmetry quadrupole, it would be possible to obtain exact first-order isochronism. However, this step would unduly complicate the system.

acceptable diameter in the radial plane for passage through the second set of bending magnets.

H. Drift Space D_3

The drift space D_3 was chosen to make the whole transport system achromatic. Given the angle of bend of B_1 and B_2 and the drift space D_2, the distance D_3 and the field of Q_2 are adjusted to cause the elements $(x|\delta_o)$ and $(\theta|\delta_o)$ of the total transformation matrix to vanish at the exit of the second bending magnet, B_2. By definition the system is then achromatic. This property makes it easy to transport the beam over the remaining distance to the end station without having the beam spread because of dispersion.

A lower limit on the length of D_3 was set by the space requirements for the slit structure and for the collimator that protects the second set of bending magnets from excessive radiation.

I. Bending Magnet B_2

The angle of bend of this magnet was chosen to be equal to that of B_1 (12^o) because this leads to the smallest loss of isochronism in the beam. This magnet also serves the important function of separating the electron beam from the off-energy and neutral background generated at the slit.

J. Quadrupole Doublet Q_3

Having removed the dispersion from the beam, it is now necessary to reduce its divergence to as small a value as possible in order to keep the beam small as it drifts to the end station. This is the function of Q_3. The quadrupoles are adjusted so that the elements $(\theta|\theta_o)$ and $(\varphi|\varphi_o)$ of the transformation matrix between the slit and the exit face of Q_3 are essentially zero. This yields a nearly parallel beam which can drift several hundred meters without expanding appreciably.

K. Drift Space D_4

As a result of the action of Q_3, this distance can be extended several hundred meters, if desirable, without the beam becoming more than a few centimeters in diameter. Essentially, the transport system up to

This point has traded beam size for divergence, the phase volume being kept constant.

L. Quadrupole Doublet Q_4

Somewhere prior to the target this doublet is inserted in the beam to focus it down to the desired spot size or to phase-match the beam to an experiment.

M. Drift Space D_5

This distance is chosen in conjunction with the gradients of Q_4 to give the desired spot size or the proper phase match into an experiment or an auxiliary system. For the distance chosen, a spot size of the order of one square millimeter is possible. The corresponding divergence is 3×10^{-4} radians from phase space conservation. The closer the doublet is to the target, the smaller will be the spot size that can be achieved.

IV. RESULTS OF FIRST-ORDER DESIGN CALCULATIONS

The elements of the system shown in Fig. 1, together with the optical requirements imposed on the system in the last two sections, were read into TRANSPORT.[2] The results of the computer run are presented in Fig. 3 and in Tables I and II.

Table I gives the magnet parameters and drift distances for the system. Table II contains the data needed to draw a floor layout of the system. The last three pairs of columns give the X, Y and Z coordinates of the vertex* of the magnet in that row. The coordinate system

*The vertex is the point of intersection of the extended beam lines from the entrance and exit faces of the magnet (see drawing below). The center lies on the magnetic axis in the middle of the magnet. For a quadrupole the center and vertex coincide. The

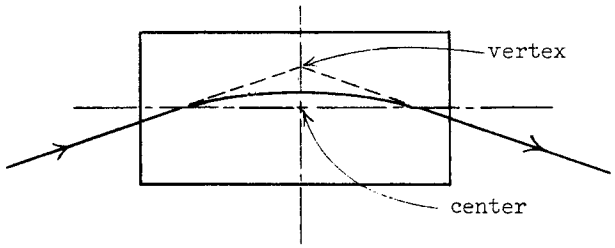

rectangular bending magnets will be positioned so that an electron following the central trajectory will stay near the magnetic axis, i.e., such that

$$\int_{-\theta/2}^{\theta/2} d^2(\theta')d\theta'$$

is a minimum (d is the distance of the central trajectory to the magnetic axis and θ is the angle of bend). A nominal value for the distance between vertex and center is $L \cdot \theta/6$ (L is the effective length of the magnet), or about 2.6 cm for switchyard magnets.

TABLE I

SYSTEM A PARAMETERS (25 GeV/c)

	Element Type	Magnetic Length (meters)	Field at Pole (kG)	Bore (2a) (cm)	Pole Rotation β_1 (deg) β_2
P	Bend*	7.0	1.04 (1.774)		0, 0.5
D_1	Drift	78.5			
Q_1a	Quad	2.0	-1.661	8.0	
	Drift	2.0			
Q_1b	Quad	2.0	1.739	8.0	
	Drift	1.5			
B_1a	Bend	3.0	14.55		1.5, 1.5
	Drift	1.5			
B_1b	Bend	3.0	14.55		1.5, 1.5
	Drift	2.0			
B_1c	Bend	3.0	14.55		1.5, 1.5
	Drift	9.25			
B_1d	Bend	3.0	14.55		1.5, 1.5
D_2	Drift	15.76			
Q_2	Quad	2.0	2.393	18.6	
D_3	Drift	21.99			
B_2a	Bend	3.0	14.55		1.5, 1.5
	Drift	1.5			
B_2b	Bend	3.0	14.55		1.5, 1.5
	Drift	1.5			
B_2c	Bend	3.0	14.55		1.5, 1.5
	Drift	1.5			
B_2d	Bend	3.0	14.55		1.5, 1.5
	Drift	1.5			
Q_3a	Quad	2.0	1.421	8.0	
	Drift	2.0			
Q_3b	Quad	2.0	-1.285	8.0	
D_4	Drift	Variable			

The last elements in the system have not been specified as yet

*The pulsed bending magnet actually consists of five magnets each having a magnetic length of 0.82 meters. They are mounted on a frame, the whole configuration being 7 meters long. The field given in parentheses corresponds to 4.1 meters of magnet, not 7.

TABLE II

SYSTEM A LAYOUT

	Element Type	Effective Length (meters)	Bend Angle (deg)	Total Length Along CT (meters)	Total Bend Angle (deg)	Coordinates of Vertex of Magnet X (meters)	X (feet)	Y (meters)	Y (feet)	Z (meters)	Z (feet)
P	BEND	7.00	.50	7.00	.50	.00	.0	-.02	-.1	3.50	11.5
D_1	DRIFT	78.50		85.50	.50						
Q_1	QUAD	2.00		87.50	.50	.72	2.4	-.40	-1.3	86.50	283.8
	DRIFT	2.00		89.50	.50						
	QUAD	2.00		91.50	.50	.76	2.5	-.42	-1.4	90.50	296.9
	DRIFT	1.50		93.00	.50						
B_1	BEND	3.00	3.00	96.00	3.50	.79	2.6	-.44	-1.4	94.50	310.0
	DRIFT	1.50		97.50	3.50						
	BEND	3.00	3.00	100.50	6.50	1.07	3.5	-.46	-1.5	98.99	324.8
	DRIFT	2.00		102.50	6.50						
	BEND	3.00	3.00	105.50	9.50	1.63	5.4	-.48	-1.6	103.96	341.1
	DRIFT	9.25		114.75	9.50						
	BEND	3.00	3.00	117.75	12.50	3.66	12.0	-.51	-1.7	116.04	380.7
D_2	DRIFT	15.76		133.51	12.50						
Q_2	QUAD	2.00		135.51	12.50	7.61	25.0	-.55	-1.8	133.87	439.2
D_3	DRIFT	21.99		157.50	12.50						
B_2	BEND	3.00	3.00	160.50	15.50	12.91	42.3	-.61	-2.0	157.78	517.6
	DRIFT	1.50		162.00	15.50						
	BEND	3.00	3.00	165.00	18.49	14.11	46.3	-.62	-2.0	162.11	531.9
	DRIFT	1.50		166.50	18.49						
	BEND	3.00	3.00	169.50	21.49	15.54	51.0	-.63	-2.1	166.38	545.9
	DRIFT	1.50		171.00	21.49						
	BEND	3.00	3.00	174.00	24.49	17.18	56.4	-.63	-2.1	170.57	559.6
	DRIFT	1.50		175.50	24.49						
Q_3	QUAD	2.00		177.50	24.49	18.84	61.8	-.63	-2.1	174.21	571.6
	DRIFT	2.00		179.50	24.49						
	QUAD	2.00		181.50	24.49	20.50	67.3	-.63	-2.1	177.85	583.5
D_4	DRIFT	201.50		383.00	24.49						
	QUAD	2.00		385.00	24.49	104.86	344.0	-.63	-2.1	363.04	1191.1
	DRIFT	2.00		387.00	24.49						
	QUAD	2.00		389.00	24.49	106.52	349.5	-.63	-2.1	366.68	1203.0
	DRIFT	15.00		404.00	24.49						

64-1-A

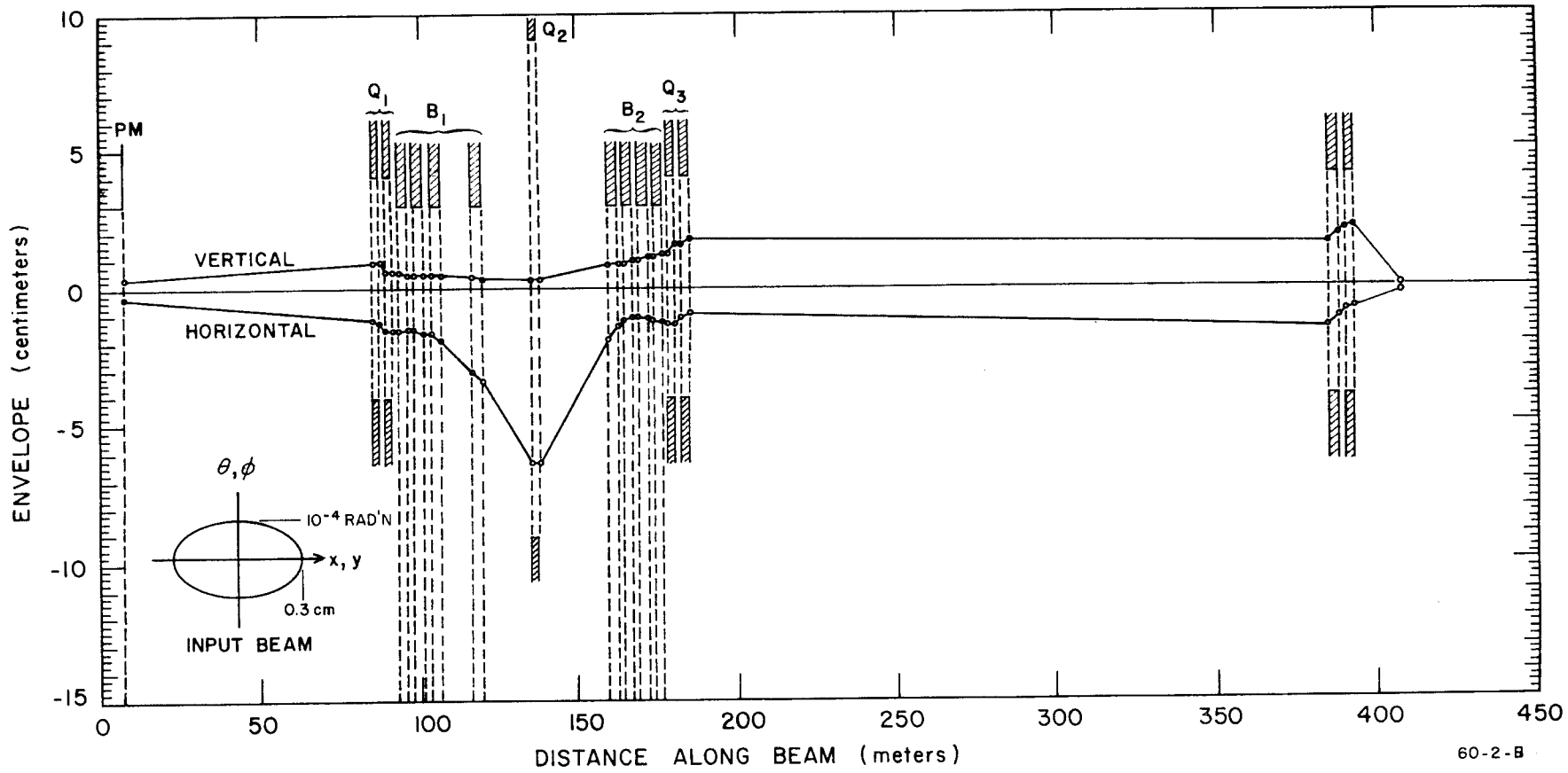
10
5
0
-5
-10
-15
ENVELOPE (centimeters)
PM
Q1
B1
Q2
B2
Q3
VERTICAL
HORIZONTAL
θ,φ
10⁻⁴ RAD'N
x, y
0.3 cm
INPUT BEAM
0
50
100
150
200
250
300
350
400
450
DISTANCE ALONG BEAM (meters)
60-2-8

FIGURE 3

has its origin at the ABA coordinate designation 101 + 75, which is approximately the center of the entrance face of the switching magnet. The Y-axis is vertically up, the Z-axis is the projection of the beam direction onto the horizontal plane, and the X-axis completes a right-handed system.

A. Envelope

Figure 3 displays the envelope of the beam as it passes through the system. The envelope of the vertical plane is drawn above the center line; the horizontal plane is shown below. The cross-hatched lines locate the magnets and the dotted portion of the magnets above and below the center line indicates the magnet aperture in the respective planes. For example, the symmetry quadrupole, labled Q2, is two meters long and has equal horizontal and vertical bore radii, 9.3 cm.

The beam envelope traced out in Fig. 3 is the envelope of all electrons whose initial coordinates lie within the six-dimensional ellipsoid whose semi-axes are: $x_o = 0.3$ cm, $\theta_o = 10^{-4}$ rad, $y_o = 0.3$ cm, $\varphi_o = 10^{-4}$ rad, $z_o = 0.3$ cm, and $\delta_o = 1.0$ percent. To appreciate more fully the meaning of this last statement, consider the three-dimensional phase volume of Fig. 4a. The semi-axes of the three-dimensional ellipsoid are x_o, θ_o, and δ_o. If the initial coordinates of a particular electron are denoted by $(x_o, \theta_o, \delta_o)$, then the extreme rays contained in this phase volume are: $(\pm x_o, 0, 0)$, $(0, \pm\theta_o, 0)$ and $(0, 0, \pm\delta_o)$. These rays are pictured in Fig. 4b. Also shown (dotted) is the ray $(x_o, \theta_o, \delta_o)$. This ray is not contained in the ellipsoidal phase volume, nor is its behavior accounted for in the envelope drawn in Fig. 3. If this ray, which corresponds to one vertex of the rectangular parallelepided, is of interest, then the parallelepided can be inscribed by an ellipsoid whose semi-axes are $\sqrt{3}$ times those of the parallelepiped and the resulting ellipsoid can be traced through the system. This procedure will produce an envelope whose extent is $\sqrt{3}$ times that of the envelope in Fig. 3

B. Ray Trace

To investigate the problem of extreme rays more conventionally, the electrons whose coordinates represent the vertices of the parallelepiped

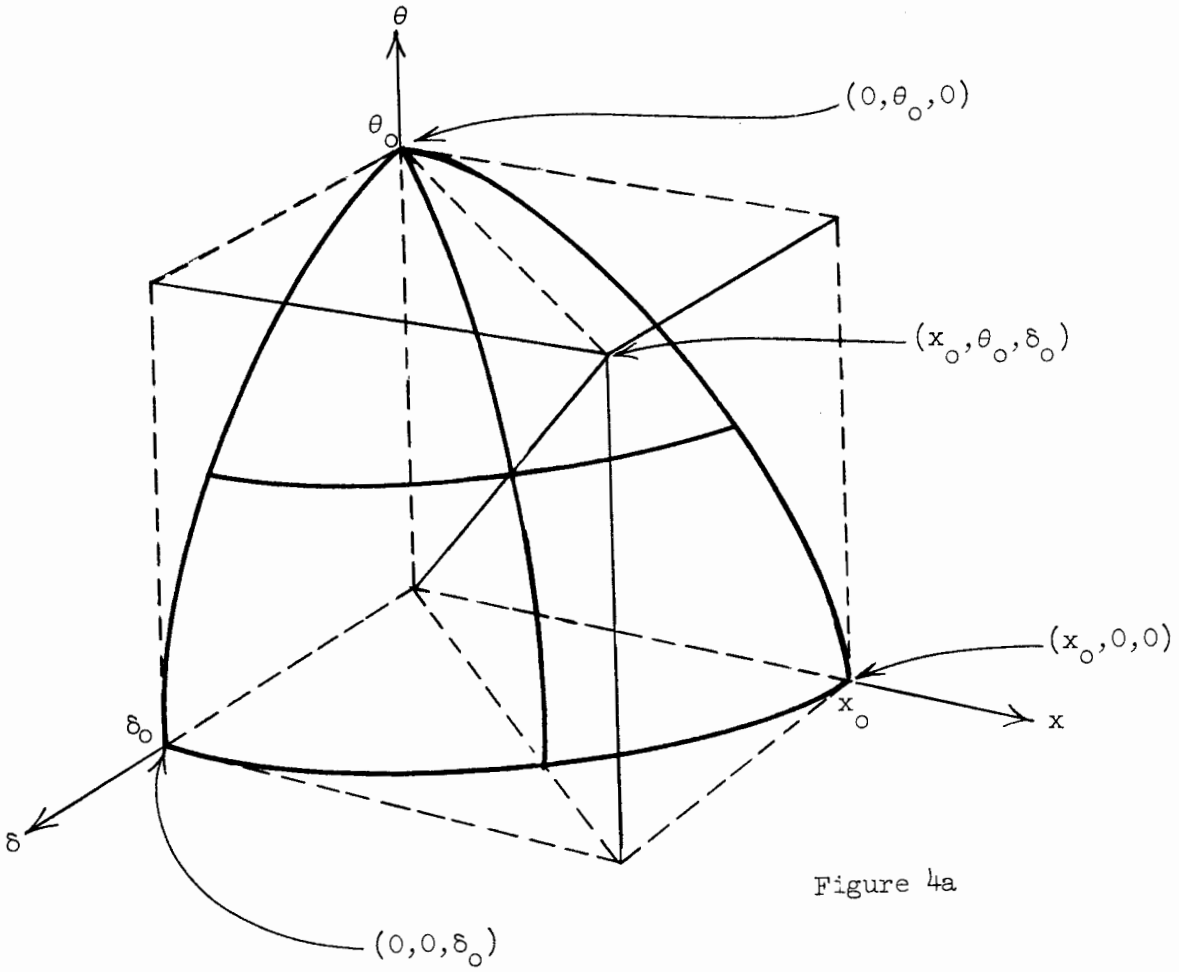

Figure 4a

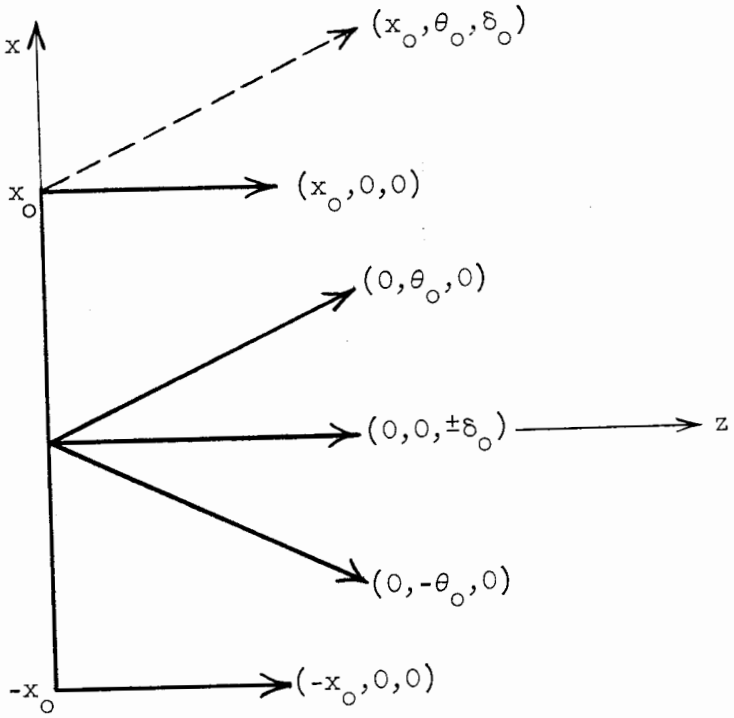

Figure 4b

in Fig. 4a were ray-traced through the system. The results are presented in Table III, with the exception of the central ray (0, 0, 0). It is seen that the first ray, which corresponds to $(x_o, \theta_o, \delta_o)$, stays within the magnet apertures everywhere in the system, although it does reside outside the envelope in most places. This table should clarify the interpretation of the envelope of an initial phase volume. All particles whose coordinates lie within the initial phase volume stay within the volume as it is transformed through the system and within the envelope traced out by the volume (for example, rays 5, 6, and 7). Those particles with initial coordinates outside the initial phase volume stay outside the transformed volume but may dip inside the envelope (see rays 1, 2, 3 and 4), but if they do, they will have a divergence which puts them outside the phase volume.

C. Apertures

The apertures necessary to pass all those electrons in the specified phase volume can be read from the envelope. They are given in Table IV together with the apertures chosen for the magnets. From the ray traces in Table III it can be seen that these apertures will pass the parallelepiped phase volume pictured in Fig. 4a with one or more centimeters to spare. The horizontal apertures of the bending magnets were made especially large to insure a flat field across the central portion of the magnet.

D. Resolution

The transformation matrix from the front face of the switching magnet to the exit face of the symmetry quadrupole contains the pertinent information concerning the first-order resolution of the perfectly aligned system. The smallest momentum interval that this system can define (with a zero width slit) is given by

$$\delta_{min} = \frac{m\, x_o}{D}$$

where m is the horizontal magnification of the system between the source and the slit [this is given by (x/x_o)], x_o is the initial object size (collimator radius, for example), and D is the dispersion of the system

TABLE III

RAY TRACE FOR SYSTEM A*

		Entrance to Q1	Entrance to B1	Exit of B1	Slit	Entrance to B2	Exit of B2	Exit of Q3	End of D4	Target
Envelope	H	1.15cm	1.60cm	3.46cm	6.33cm	1.86cm	1.19cm	0.97cm	1.49cm	0.06cm
	V	0.91cm	0.57cm	0.24cm	0.24cm	0.80cm	1.20cm	1.79cm	1.51cm	0.02cm
Ray**										
1. (.3,1,1)	H	1.87	2.59	4.02	6.23	0.84	-1.48	-1.19	-1.24	0.07
	V	1.15	0.71	0.16	-0.24	-1.03	-1.58	-2.38	-2.11	0.00
2. (.3,1,0)	H	1.15	1.58	0.60	-0.10	-0.89	-1.48	-1.19	-1.23	0.07
	V	1.15	0.71	0.16	-0.24	-1.03	-1.58	-2.38	-2.11	0.00
3. (0,1, 1)	H	1.57	2.19	3.92	6.33	1.08	-1.15	-0.94	-1.48	0.01
	V	0.85	0.54	0.23	0.00	-0.28	-0.47	-0.72	-0.90	-0.02
4. (.3,0,1)	H	1.02	1.39	3.52	6.23	1.50	-0.33	-0.26	0.23	0.06
	V	0.30	0.16	-0.07	-0.24	-0.75	-1.11	-1.64	-1.21	0.01
5. (0,1,0)	H	0.85	1.19	0.50	0.00	-0.65	-1.15	-0.94	-1.47	0.01
	V	0.86	0.54	0.23	-0.00	-0.28	-0.47	-0.72	-0.90	-0.02
6. (.3,0,0)	H	0.30	0.39	0.10	-0.10	-0.23	-0.33	-0.25	0.25	0.06
	V	0.30	0.16	0.07	-0.24	-0.75	-1.10	-1.64	-1.21	0.01
7. (0,0,1)	H	0.72	1.00	3.42	6.33	1.73	0.00	0.00	0.00	0.00
	V	0.00	0.00	0.00	0.00	0.00	0.00	0.00	0.00	0.00

*Table entries are position of ray at the location indicated.

**The values correspond to (x_o cm, $\theta_o \times 10^{-4}$ rad, δ_o percent) in the radial plane and (y_o, φ_o, δ_o) in the vertical plane.

at the slit [this is given by (x/δ_o)]. The ultimate resolution for system A is:

$$\delta_{min} = \frac{0.335 \times 0.3}{6.33} = \pm 0.015\%$$

The slit width, w, which passes a given momentum interval, δ, is given by

$$w = \pm 6.33\ \delta \text{ cm}$$

where δ is in percent. For

$$\delta = \pm 0.05\%,$$

$$w = \pm 0.316 \text{ cm}$$

The distribution of momenta through a slit w that allows δ percent to pass through is shown in Fig. 5. If $\delta = 0.05$ percent, then all particles with momenta between ±0.035 percent pass through the slit, half those with momenta between ±0.05 percent get through, and no particles with momenta greater than ±0.065 percent survive the slit.

TABLE IV

APERTURE REQUIRED

	Aperture		Bore Radius Chosen (Available Aperture)	
	Horizontal	Vertical	Horizontal	Vertical
Doublets	1.85 cm	1.32 cm	± 4.0 cm (± 3.65)	± 4.0 cm (± 3.65)
Symmetry Quad	6.35	0.26	± 9.3 (±12.0)	± 9.3 (6.0)*
Bending Magnets	3.45	1.29	±15.0 (± 8.25)	± 3.0 (± 2.37, see p.33)

*A diamond-shaped vacuum pipe is used in the symmetry quad and this allows a wider horizontal aperture. The magnet has been designed to provide a good quadrupole field in this region.

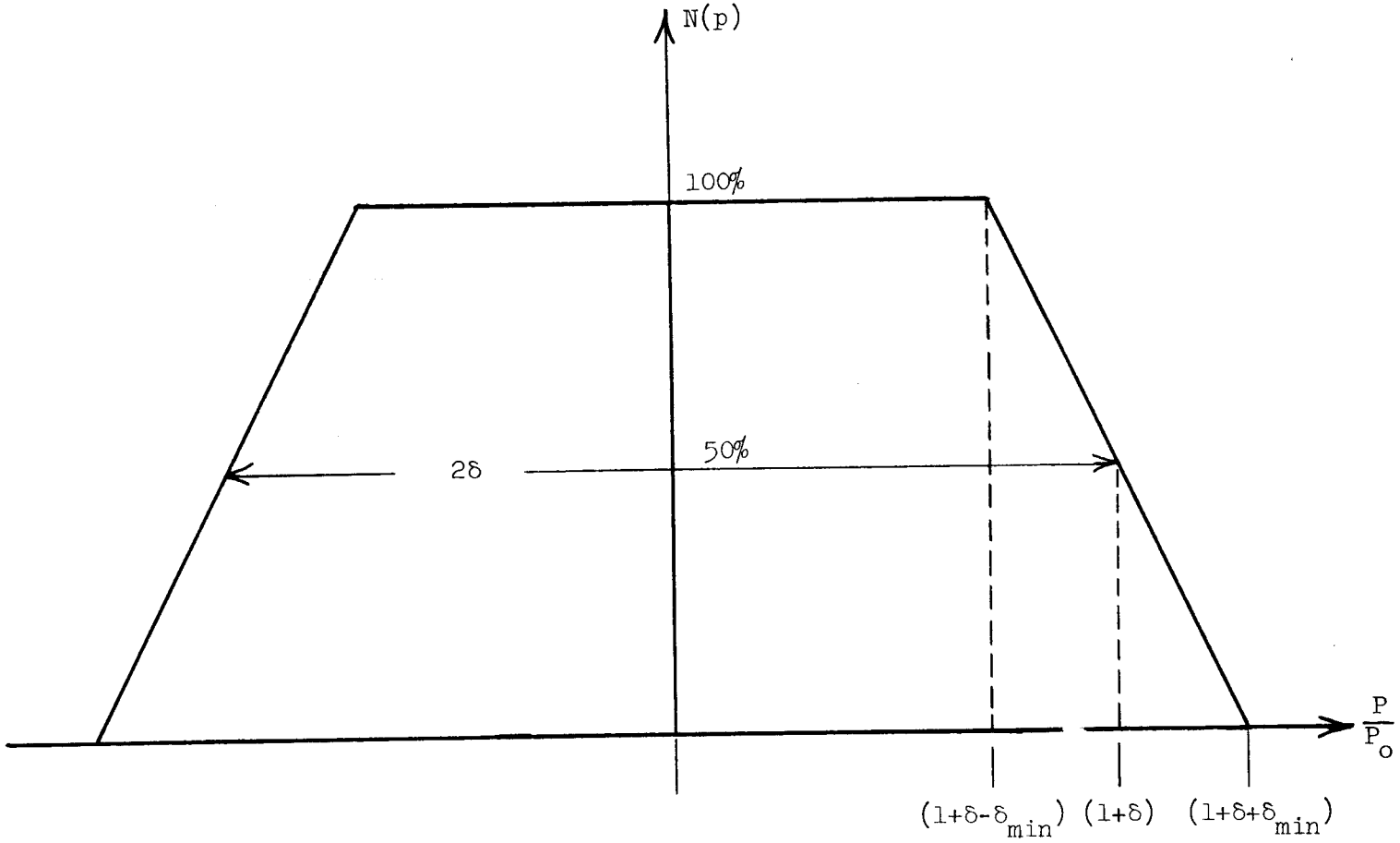

Figure 5

E. Isochronism

In passing through system A, the bunch length grows by $\pm 16^{\circ}$ in rf phase (≈ 0.49 cm). When combined with the initial bunch length, the total bunch length is still within the ± 0.6 cm or $\pm 20^{\circ}$ tolerance on the system. The growth in bunch length is entirely due to the momentum spread through the $(z|\delta_o)$ matrix element. The symmetry and achromatic properties of the system cause the $(z|x'_o)$ and $(z|\theta_o)$ elements to vanish for relativistic particles.

F. Final Spot

The beam leaving Q_3 has a very small divergence and can drift several hundred meters without becoming more than a few centimeters in diameter. A second transport system or any kind of phase matching system can be located anywhere after Q_3 and its effect on the beam will be orthogonal to system A.

For example, a quadrupole doublet Q_4 was located 200 meters after Q_3 and the beam was focused to a spot at $D_5 = 15$ meters downstream. The image dimensions obtained with modest quadrupole gradients were $x = \pm 0.6$ mm and $y = \pm 0.2$ mm. The corresponding divergences can be obtained from phase space conservation. They are 5×10^{-4} and 14×10^{-4} radians, respectively. A still smaller spot could be obtained if the final drift, D_5, were shortened and the quadrupole gradients strengthened. Conversely, larger images could be obtained by lengthening D_5 and relaxing the gradients. Finally, Q_3 and Q_4 could be operated together to match almost any system admittance desired.

G. Gamma Beam

It has been proposed[3] that a thin radiator (10^{-3} to 10^{-5} radiation lengths) be placed in the electron beam after the second bending magnet in B_1. The gamma beam created at the radiator would be brought out into an area between the center line of the accelerator and area A. The proposed gamma beam line is shown on Fig. 1. To provide clearance for this beam, the fourth magnet in B1 was moved nine meters downstream. This modification provides five centimeters clearance between the gamma beam line and the magnet yoke. This is thought to be sufficient allowance for the beam, the vacuum pipe, and any lateral shifting of the magnet to

keep the beam in its central region. Moving the magnet necessitated a 3 percent increase in the symmetry quadrupole field and a 0.5 percent change in the fields of Q_1. The ultimate resolution of the system decreased 0.5 percent to ±0.015 percent, but this is still better than required. No change in magnet apertures was necessary. The radius of the gamma beam in the vicinity of the fourth bending magnet is ±1 inch or less. After drifting 150 meters past the fourth magnet, the gamma beam has the dimensions $x = \pm 15.1$ cm by $y = \pm 2.2$ cm.

H. Tracking

System A must be able to satisfy the momentum definition tolerances over a wide momentum interval from 25 GeV/c down to one-tenth of that value. This requirement raises the question of tracking. Because all the bending magnets will be run in series, the problem divides itself into two parts--correlated and uncorrelated errors. The correlated error is the error common to all the bending magnets, namely, an error in current setting. The error in the angle of bend is related to the field (current) error by $\Delta\alpha/\alpha = \Delta B/B$, where the field B corresponds to the bend angle α. The lateral displacement of the central trajectory at the slit resulting from a correlated field error is $s = d \cdot \Delta\alpha$, where d is the distance from the slit to the center of the B_1, approximately 34 meters. A 3.2 mm half-slit width corresponds to a momentum bite of 0.05 percent. The displacement corresponding to 0.02 percent is 1.3 mm. Because 0.02 percent is the desired momentum repeatability, it is required that s be held to 1.3 mm. Thus $\Delta B/B = 1.8 \times 10^{-4}$, which is to say, the current must be controlled and able to be reset to about one part in 10,000.

Uncorrelated errors were evaluated with TRANSPORT in the following manner. The effect of an error in field ($\Delta B/B$) is identical to an error in momentum ($\Delta p/p$) of the same magnitude. An uncertainty in the value of the field causes an uncertainty in the position of the central trajectory; however, no dispersion is introduced, as would be the case if the momentum were uncertain. In TRANSPORT uncorrelated field uncertainties are treated as momentum uncertainties, and then the dispersion is erased where appropriate.

An uncertainty of 10^{-4} in the value of $\Delta B/B$ was assigned to each of the four bending magnets in B_1, and the uncertainty in the beam position at the slit was 0.03 cm. Thus the fluctuations in $\Delta B/B$ of the magnets can be as high as three or four parts in 10,000.

I. Effect of Earth's Magnetic Field

In the vicinity of Stanford University the total intensity of the earth's magnetic field is 0.514 gauss and the dip angle is 61.5 degrees. The vertical component of the earth's field is thus 0.450 gauss. This field, acting over the length of the first half of the transport system, will cause a horizontal displacement of the beam at the slit and hence an error in momentum definition.

The horizontal component, which has a strength of 0.25 gauss, causes a vertical displacement and has no effect on resolution. However, this field does cause a vertical shift in beam position in the magnet B_2.

The effect of the earth's field was simulated with TRANSPORT by replacing the major drift spaces with bending magnets whose field was equal (in strength and direction) to that of the earth's field. The table below gives the results. For comparison, the displacements are also calculated neglecting focusing properties at the switchyard by simply adding the appropriate $\int Bd\ell$ to the central trajectory. The beam energy is taken at 2.5 BeV and 25. BeV.

	2.5 BeV beam	25. BeV beam
Horizontal		
By (gauss)	0.45	0.45
actual displacement at slit (cm)	1.0	0.1
displacement neglecting focusing (cm)	2.0	0.2
Vertical		
Bx (gauss)	0.25	0.25
actual displacement at end of magnet B_2 (cm)	3.0	0.3
displacement neglecting focusing (cm)	2.2	0.22

These numbers show that sheilding and/or steering is necessary, especially for beams at low energy.

V. SECOND-ORDER ABERRATIONS

The results of the last section were based on the first-order theory of beam optics. To establish the validity of the first-order theory, it is necessary to show that all second-order aberrations are negligible or nearly so. That is the purpose of this section.

There are two types of second-order aberrations--physical and geometrical. The physical aberrations are the result of magnet imperfections, including the failure of first-order magnet parameters to describe adequately the effect of fringe fields. The geometrical aberrations are important when the linear approximations, made in first-order theory, are no longer valid. This occurs when any of the following conditions fail:

$$x/\rho \ll 1,\ \theta \ll 1,\ y/\rho \ll 1,\ \varphi \ll 1, \text{ and } \delta \equiv \Delta p/p \ll 1.$$

For system A, $x/\rho \approx y/\rho \approx 10^{-3}$, $\theta \approx \varphi \approx 10^{-4}$, and $\delta \approx 10^{-2}$. One would expect that if any second-order aberrations are important, they would be chromatic in nature, namely, dependent on δ. However, because all second-order aberrations involve products of the above quantities, it is to be expected that second-order effects are negligible for system A. This is indeed true except for magnet imperfections.

In describing the results calculated by TRANSPORT, it is first necessary to catalog all the second-order matrix elements currently in the program.

A. Quadrupoles

Three assumptions were made about the quadrupole magnets on the system: (1) There exists a straight line through the quadrupole along which the field is zero. This is the magnetic axis. (2) The potential from which the field is derived is origin-symmetric and z-independent. (3) The magnet has fringe fields which may be neglected to third order. These assumptions are sufficient to insure that all aberrations except those which are chromatic in nature vanish to third order. The second-order chromatic aberrations used in the calculation were those derived by Howry.[4]

B. Bending Magnets

The bending magnets designed for system A are the rectangular, uniform field (n=0) type. There are a host of mathematical second-order aberrations associated with this type of magnet. In addition, there is a group of physical aberrations resulting from the quadratic deviation from field uniformity, specifically, a non-zero β in the field expansion:

$$H_y(x,y) = H_o \left[1 - nx/\rho + \beta x^2/\rho^2 + (n/2 - \beta)y^2/\rho^2 + \ldots \right]$$

and

$$H_x(x,y) = H_o \left[-ny/\rho + 2\beta xy/\rho^2 + \ldots \right]$$

The matrix elements used to calculate these aberrations for radial midplane trajectories were those given by Belbeoch, Bounin and Brown.[5] The second-order coefficients for radial off-midplane trajectories were derived by Brown,[6] and independently by Howry. Howry[7] derived the coefficients for vertical midplane and off-midplane trajectories, and second-order path length effects. Some additional off-midplane coefficients associated with the rotated pole faces have been derived by Helm[8] but have not yet been incorporated into TRANSPORT. As with quadrupoles, the second-order fringe fields have been neglected.

The complexity and sheer number of the second-order matrix elements used in the calculations lead to the question of accuracy, both of derivations and of implementation into TRANSPORT. However, a recent independent check of all the terms has been performed and compared with the computer program; in addition, numerical computer calculations on some known systems have been verified.

It is felt, therefore, that the results given below represent a reasonable second-order model.

C. Geometric Aberrations

There are three criteria for judging the size and effect of second-order aberrations: The second-order aberrations must not (1) affect the resolution of the system, or (2) cause the beam to exceed the magnet apertures, or (3) cause the final spot size at the target to be appreciably enlarged. The geometrical aberrations were studied first. The

first-order solution for system A was given to TRANSPORT and the second-order mode was activated with $\beta = 0$. The largest second-order effect at the slit [caused by the $(x|\theta\delta)$ and $(x|x\delta)$ terms] is a factor of 100 smaller than the first-order magnification, which limits the resolution. All other second-order effects taken together create a number which is three orders of magnitude smaller than the magnification. There was no appreciable gain in the beam size through the magnets, the most serious increase being less than 1% of the vertical size in B_2. The target size increased from 0.06 cm horizontal and 0.02 cm vertical to 0.09 cm and 0.03 cm, respectively.

D. Magnet Imperfections

It has been assumed that bending magnets can be built so that the coefficient of the field gradient, n, is vanishingly small. If this assumption is not valid, the field gradients of the quadrupole doublet Q_1 can be adjusted to compensate. However, nothing so simple can be done for the non-vanishing quadratic coefficient, β, in the expansion of the magnetic field. A tolerance must be set on β such that the effect of aberrations relating to it will be small. The actual parameter which is determined from magnetic measurements is not β but ϵ :

$$\epsilon(x) = 1 - \frac{H_y(x,0)}{H_o}$$

where H_y is evaluated at a position x away from the central trajectory in the median plane. From the field expansion given for H_y with $n = 0$, it is seen that ϵ and β are related by

$$\beta\, x^2/\rho^2 + \ldots = \epsilon(x)$$

The function ϵ will probably be determined from measurements of $\int B d\ell$ through the magnet for various distances from the magnet centerline. The parameter β may then be fitted in a least squares sense from the above relation, neglecting terms higher than quadratic, and the β value obtained can be used to calculate the second-order effects of the magnet imperfections on the beam, with subsequent action taken to correct it if necessary.

The design of the bending magnets as it relates to the function ϵ has been discussed.* Assuming ϵ to be a quadratic function of x, it is anticipated that the value of ϵ at x = 1 cm from the magnet axis will be about 2×10^{-5}. In principle, the wide poles (±15 cm) should give a much smaller value of ϵ, but based on past comparisons between designed and measured values, the above value seems reasonable.

The second-order beam envelope for system A, with ϵ a pure quadratic function, and various values of $\epsilon_1 \equiv \epsilon(x)\Big|_{x=1 \text{ cm}}$ were calculated by TRANSPORT. The values chosen were $\epsilon_1 = 0$, 2×10^{-5}, and 10^{-4}. For $\epsilon_1 = 10^{-4}$, the calculations showed that the most serious change is an increase in vertical beam size to 1.27 cm at the end of the last magnet of B_2. This is still within the specified apertures. All other increases in beam size are less than 5% for $\epsilon_1 = 10^{-4}$.

At the slit magnet, imperfections increase the size of all the aberrations. The position x of the electrons at the slit as a function of δ is shown schematically in Fig. 6.

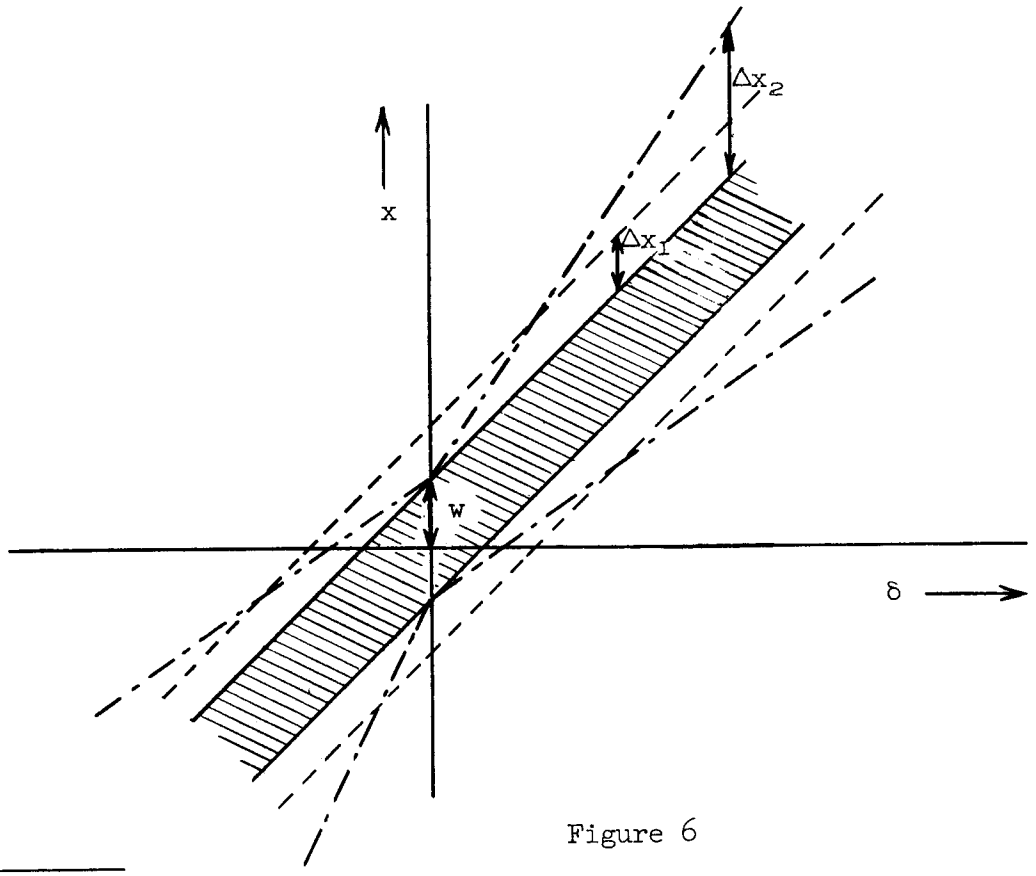

Figure 6

*B. Hedin, private communication.

The vertical half-width w of the shaded band is 0.1 cm, a consequence of first-order magnification and the non-zero initial spot size. The cumulative effect of all the δ-independent second-order coefficients, e.g. $(x|x^2)$ and $(x|x\theta)$, is to widen the shaded band by an amount $2\Delta x_1$ (as indicated by the dotted lines in Fig. 6). The cumulative effect of the chromatic second-order terms, $(x|x\delta)$ and $(x|\theta\delta)$, is to re-form the band into a cone (dashed lines) whose half-width at $\delta = 0.5\%$ has grown to $(\Delta x_2 + w)$. It should be noted that the density of particles near the new edge of the band is probably much smaller than at the center. For example, particles at the upper edge must have positive initial x, θ, y and negative φ, whereas any combination of signs is possible near the center of the band.*

The values of $\Delta x_1/w$ and $\Delta x_2/w$ affect the resolution of the system, and are given in Table V below. A pessimistic approximation to the second-order ultimate resolution is $\delta_{min} = \delta_{min}[\text{first order}](1 + \Delta x_1/w)$. The values show that the second-order effects are negligible if the horizontal beam divergence from the accelerator is 10^{-5} radians but are somewhat detrimental at 10^{-4} radians.

TABLE V

	Original horizontal beam divergence = 10^{-4}		Original horizontal beam divergence = 10^{-5}	
	$\frac{\Delta x_1}{w}$	$\frac{\Delta x_2}{w}$ at $\delta = 0.5\%$	$\frac{\Delta x_1}{w}$	$\frac{\Delta x_2}{w}$ at $\delta = 0.5\%$
$\epsilon_1 = 0$	.002	.16	.0002	.04
$\epsilon_1 = 2 \times 10^{-5}$	.25	.38	.024	.12
$\epsilon_1 = 10^{-4}$	1.23	1.21	.12	.38

A second effect of ϵ is that it causes a different mean momentum to pass through the slit. This can be seen from Fig. 7. Three electrons

*This points out the futility of excessive investigation into higher order effects without knowledge of the initial beam distribution.

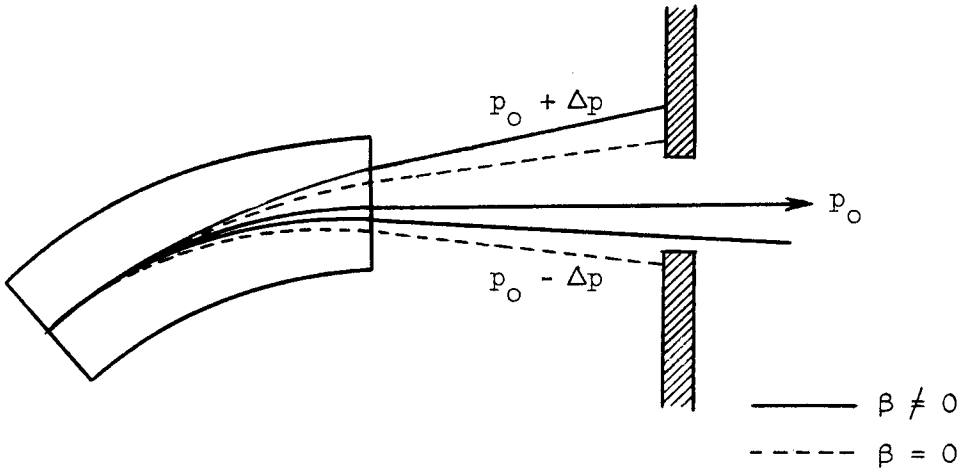

Figure 7

with momenta $p_o + \Delta p$, p_o, and $p_o - \Delta p$ enter a bending magnet perpendicularly on the magnetic axis. The electron with momentum p_o follows the same trajectory regardless of the value of β. The electron with momentum $p_o + \Delta p$ bends away from the centerline; because the field decreases parabolically with the radius, the electron passes through an even weaker field and is bent less than calculated in first order. As a result, the electron follows the solid trajectory rather than the dashed one. Similarly, the $p_o - \Delta p$ electron does not pass through as strong a field and is also bent less than would be expected in first order, and it, too, follows the solid line. The net result averaged over a distribution of momenta is that the mean momentum passing through the slit is not p_o but some smaller value. This effect is described by the $(x|\delta_o^2)$ aberration. At the slit its value is 0.176 cm/%^{2} for $\epsilon_1 = 10^{-4}$.

The position of the electrons at the slit as a function of δ is again shown in Fig. 8. The half-width of the shaded band is 0.1 cm, as before. The effect of the $(x|\delta^2)$ term is to bend the region into a parabola (dotted lines), so that the displacement Δx_3 at $\delta = 1\%$ is

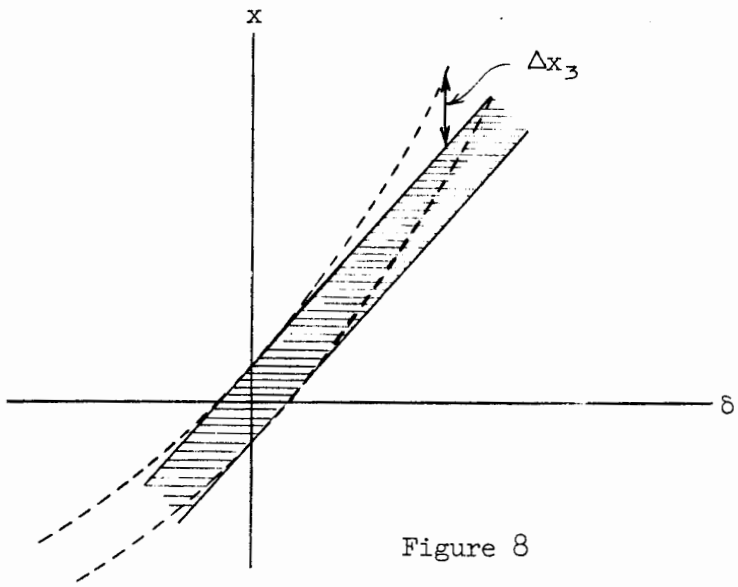

Figure 8

0.176 cm, more than the width of the band itself. It is seen that as the slits are closed, the resulting effect upon the resolution becomes less important, and is negligible for momentum bites of less than 0.5%.

The increase in target spot size as a result of second-order magnet imperfections is shown in the table below. The estimated spot sizes and displacements assume the input phase ellipsoid of Fig. 4a.

	first order	second order $\epsilon_1 = 0$	$\epsilon_1 = 2 \times 10^{-5}$	$\epsilon_1 = 10^{-4}$
est. x spot size	.06	.09	.11	.25
est. y spot size	.02	.03	.04	.04
mean x displacement	0	-.02	-.03	-.14
mean y displacement	0	0	0	0

Figure 9 shows where a few rays, chosen at random from the faces of the cube of Fig. 4a, will hit the target. The value of ϵ_1 is taken as 10^{-4}.

The only detectable second-order effect upon isochronism is a small lag of off-momentum particles behind the reference particle, due to the greater distance traveled by the former. The centroid of the bunch lags the reference particle by .05 cm (about 1.6° in rf phase) at the

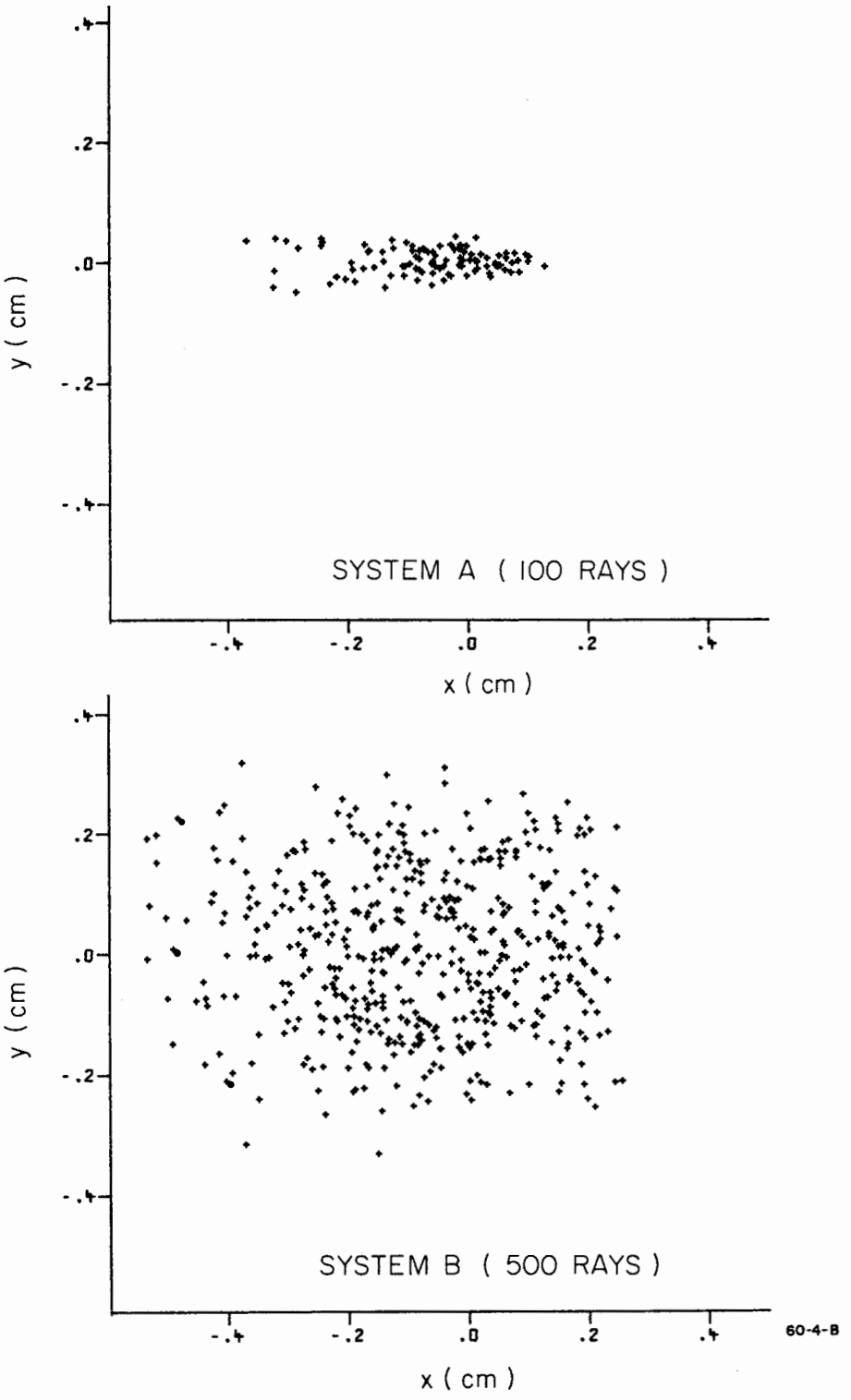

FIG. 9--Rays chosen at random from the faces of the hypercube described in Sec. VI-B are traced through the systems to second order, and their positions at the target are shown. The magnet inhomogeneity parameter ϵ_1 (see Sec. V) is taken to be 10^{-4}.

target. The bunch length increase (about the centroid) is the same as in first order.

E. Corrections

There are ways of correcting second-order aberrations. Sextapole magnets (or a 3θ correction to the quadrupole field) and curved pole tips on bending magnets give rise to second- and higher-order effects but no first-order effects. By adjusting the field of one or more sextapole magnets located at appropriate places in the system or by choosing the proper radii of curvature for the pole tips on one or more of the bending magnets, it should be possible to eliminate one or more of the second-order aberrations and substantially reduce still others. As of this writing no effort has been made to implement this corrective procedure, but it would be a worthwhile endeavor.

VI. ALIGNMENT TOLERANCES

The first- and second-order solutions discussed in the last two sections are based on the assumption that there exists through the system a reference trajectory along which the reference particle, $(x,\theta,y,\varphi,z,\delta) = (0,0,0,0,0,0)$, can travel without deviation. It is further assumed that the reference particle does indeed travel along the reference trajectory. However, in practice the magnets of the system will not be positioned exactly, nor will the initial beam be injected with precisely the correct position and direction. Thus the reference particle will not necessarily traverse the reference trajectory as assumed. This deviation from theory raises the question: What are the effects of misalignments of the initial beam and the magnets comprising the transport system upon the final beam?

A. Method of Investigation

Only first-order alignment errors are considered in this report.

There are two distinct approaches to the problem of misalignments. In the first it is assumed that the magnet suffers a differential misalignment both in its position and in its orientation with respect to the local level. In this case the reference particle would not enter on the magnetic axis and would suffer whatever focusing action the magnet provides. If the displacement of the magnet is known, the effect of the focusing as well as the position of the reference particle as it leaves the magnet can be computed, and the displacement of the magnet could be corrected.

The objection to the above approach is that in practice the displacement of the magnet from its ideal location is unknown. This uncertainty in the location of the magnet leads to an uncertainty in the position of the reference particle. It is the relation between these uncertainties and the cummulative effect of uncertainties in the position of each magnet in the system that is of primary concern.

It should be made explicit here that since positioning errors are the result of measuring errors, it is appropriate to represent the uncertainties in magnet positioning by a Gaussian distribution function.

To aid in discussing the alignment problem, the following definitions are made. A displacement of x mils means that the location of the center of the magnet was uncertain to x mils. The magnet was not actually displaced by a definite amount, but rather its location was assigned a Gaussian distribution of displacements whose standard deviation was x mils. Similarly, a rotation of x milliradians about a given axis means that the orientation of the magnet was uncertain to x milliradians about that axis.

In simulating the effect on the system of misaligning a particular magnet, the magnet was misaligned by each of the six possible errors (three displacements and three rotations) independently, and the effects on the central trajectory at strategic points of the system downstream from the magnet were tabulated. Each entry has the following interpretation: An uncertainty of m mils (or m milliradians) in the location (or rotation) of the magnet in the given direction (or about the given axis) gives rise to an uncertainty in the location of the central trajectory of x centimeters. The results below are, in effect, a table of derivatives giving the uncertainty in the location of the central trajectory per unit error for the magnet or group of magnets. The effects resulting from various alignment uncertainties combine as the sum of the squares when the errors are assigned from a gaussian distribution.

The key to the location codes used in the tables is given below.

D1 indicates the end of drift space D_1. (See Fig. 1)
Q1 indicates the exit face of doublet Q_1.
B1 indicates the exit face of bending magnet B_1.
Slit indicates the exit face of quadrupole Q_2.
D3 indicates the end of drift space D_3.
B2 indicates the entrance face of doublet Q_3.
D4 indicates the end of drift space D_4.
Target indicates the end of drift space D_5.

The coordinate system used is one in which the z axis points in the direction of the beam. The x-y plane is perpendicular to the beam direction and oriented to form a right-handed system with z. The coordinate x measures horizontal (radial) displacements while y measures vertical displacements.

B. Alignment Criteria

The two main concerns in establishing alignment tolerances on the system are apertures and resolution. The displacement of the reference axis of the beam must be kept small enough to insure that the beam does not strike any magnet aperture and that no significant deterioration occurs in the momentum defining ability of the system. For system A, these requirements amount to controlling the horizontal displacement of the beam at the slit and the vertical displacement of the beam at the exit of the second set of bending magnets (location B2).

A radial displacement of the central trajectory at the slit corresponds to passing a different mean momentum through the slit. The dispersion at the slit is 6.33 cm/percent, so that a momentum bite of ±0.05% will pass through a ±0.32-cm slit. If this resolution is to be reproducible to ±0.02% over long periods of time, then alignment errors must not shift the central trajectory in excess of $6.33 \times 0.02 = 0.13$ cm.

On exiting from the second 12° bend, the beam has a radius of 1.2 cm in the vertical plane. Because the available vertical magnet aperture is only ±2.37 cm (see Table IV), the central trajectory should not stray more than 0.67 cm if 0.5 cm is kept for a safety factor. As will be seen, four different alignment errors contribute to a vertical displacement at B2. Since the displacements add as to the sum of the squares, it would be expected that the total allowed displacement for any one error should be reduced by $\sqrt{4}$. However, two of the alignment errors are easily controlled (their alignment derivatives are relatively small), so that their effect may be neglected. Thus the total vertical displacement that can be tolerated is fixed at $0.67/\sqrt{2} = 0.46$ cm.

C. Switching Magnet, P

Table VI gives the alignment derivatives for the switching magnet. As can be seen, misalignments of the switching magnet cause negligible effects on the beam. A z displacement of any bending magnet introduces a radial displacement of the central trajectory (see figure), so the tolerance is set at 0.2 cm. The y-displacement tolerance is set at one

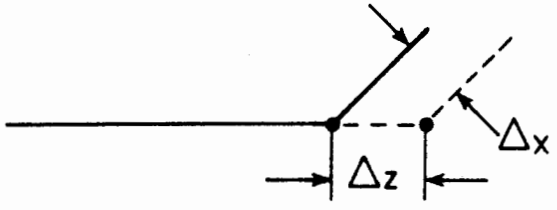

180-1-A

TABLE VI

ALIGNMENT DERIVATIVES FOR SWITCHING MAGNET P

Misalignment Type	Misalignment Axis	Axis	Uncertainty Magnitude at Location							
			D1	Q1	B1	Slit	D3	B2	D4	Target
Disp	x	x	.000 cm/mm	.000 cm/mm	.000 cm/mm	.000 cm/mm	.000 cm/mm	.000 cm/mm	.000 cm/mm	.000 cm/mm
Disp	y	y	.000	.000	.000	.000	.000	.000	.000	.000
Disp	z	x	.001	.001	.000	.000	.001	.001	.000	.000
Rotn	x	y	.000 cm/mr	.000 cm/mr	.000 cm/mr	.000 cm/mr	.000 cm/mr	.000 cm/mr	.000 cm/mr	.000 cm/mr
Rotn	y	x	.000	.000	.000	.000	.000	.000	.000	.000
Rotn	z	y	.070	.050	.020	.000	.020	.040	.010	.000

centimeter to keep the beam within the vertical aperture of P itself. The other displacement tolerance is set arbitrarily at one centimeter. The z-rotation tolerance is chosen to keep the beam within the vertical aperture of the second set of bending magnets: $0.46/0.04 \times 3 = 3.7$ mr. This must be reduced to 3 mr because of the tighter vertical displacement allowance of System B (see Section VII). The extra factor of 3 is imposed to relax the tolerances on B_1 and Q_1. Even so, the resulting tolerance of 3.0 mr is easily met. The other two rotation tolerances are set arbitrarily at 20 mr. These tolerances hold for the switching magnet taken as a whole or for the individual elements of the magnet.

Tolerances on Switching Magnet P

Axis	Translation	Rotation
x	[1. cm]	[20. mr]
y	1. cm	[20. mr]
z	0.2 cm	3.0 mr

Brackets [] indicate that the tolerance was set more or less arbitrarily.

D. Quadrupole Doublet Q_1

Before setting alignment tolerances on the doublet Q_1, a choice must be made regarding the way in which the alignment process is to be done. The two quadrupole magnets could be aligned separately in the system; this would require a set of tolerances on the alignment of each magnet. Alternatively, the pair of magnets could be aligned on a rigid frame and the frame aligned in the system. This process would require one set of tolerances for aligning the magnets on the frame and a second set of tolerances for aligning the doublet (considered as a unit) in the system. In the Appendix it is shown that the collinearity tolerance on aligning the magnet axes of the two quadrupoles on the frame is several mils, so that the frame must be leveled within 0.02 to 0.05 milliradians in order to preserve resolution and avoid magnet pole tips. Hence it was decided that the two magnets should be aligned separately. The table below gives the alignment derivatives assuming both magnets to have the same uncertainties in position.

Misalignment Type	Misalignment Axis	Axis	Uncertainty Magnitude at Location				
			Slit	D3	B2	D4	Target
Disp	x	x	.012 cm/mil	.002 cm/mil	.008 cm/mil	.054 cm/mil	.008 cm/mil
Disp	y	y	.020	.056	.084	.132	.0

There are no first-order effects resulting from a differential displacement of quadrupole elements in the z-direction or from a differential rotation about the z-axis. The misalignments were performed about the center of the magnet.

To preserve resolution, it is necessary to hold the x-displacement tolerance to 0.13/0.012 = 10 mils. In the vertical plane the beam must not strike the second set of bending magnets. This fixes the y-displacement tolerance at 0.46/0.084 = 5 mils. The z-displacement tolerance is set at 4 cm to preserve the focus condition and thus protect resolution.

The effect of rotational errors is negligible. The principal planes of a quadrupole singlet are near the center of the magnet, and a rotation of the magnet about its center does not appreciably disturb the location of the principal planes. Therefore, the rotational tolerances on the individual quadrupoles are quite relaxed, provided that the rotations are about axes fixed at the center of the magnet. They are more or less arbitrarily set at 1 milliradian, which is readily attainable and which will allow the beam to pass through the 2-meter-long quadrupoles with a loss in effective aperture of only 0.1 cm.

Tolerances on Independent Quads in Q_1

Axis	Translation	Rotation
x	10. mils	[1 mr]
y	5. mils	[1 mr]
z	[4. cm]	20. mr

E. Bending Magnets B_1

Misalignment Type	Misalignment Axis	Uncertainty Axis	Uncertainty Magnitude at Location				
			Slit	D3	B2	D4	Target
Disp	x	x	.000 cm/mm	.000 cm/mm	.000 cm/mm	.000 cm/mm	.000 cm/mm
Disp	y	y	.006	.018	.027	.040	.000
Disp	z	x	.010	.005	.015	.052	.006
Rotn	x	y	.000 cm/mr	.001 cm/mr	.001 cm/mr	.002 cm/mr	.000 cm/mr
Rotn	y	x	.000	.000	.000	.000	.000
Rotn	z	y	.38	1.11	1.58	2.36	.01

In preparing this table, all four bending magnets comprising B_1 were given the alignment uncertainty associated with a particular line in the table, and the resulting uncertainty in the location of the central trajectory at various points downstream was tabulated. It was assumed that the magnets were mounted independently so that the uncertainties were not correlated. The misalignments were done about the "center" of each magnet--a point midway along the central trajectory through the magnet.

A z-displacement of the bending magnets causes a radial displacement of the central trajectory at the slit. Preservation of resolution requires that the uncertainty in the longitudinal placement of the magnets be held to $0.13/3 \times 0.01 = 4$ mm. The extra factor of 3 was inserted to relax the tolerances on the doublet Q_1.

The z-rotation tolerance is fixed by the vertical aperture of the second set of bending magnets, B_2. The tolerance is $0.46/1.58 = 0.33$ mr. If steering is permitted, this tolerance could be relaxed and a new one calculated by considering the beam in the vicinity of the slit. The beam has a radius of 0.24 cm there, and the spectrum analyzer has a vertical aperture of ± 2 cm. The central trajectory could be off by about 1.25 cm. The z-rotation tolerance with steering would then be $1.25/0.38 = 3.3$ mr.

The x-displacement tolerance can only be fixed by requiring that the beam stay in the central portion of the bending magnet where the field is flat. This tolerance is arbitrarily set at one centimeter.

The y-displacement tolerance is set by requiring that the beam not strike the poles. Since the radius of the beam in the vertical

plane never exceeds 1.2 cm, and the central trajectory strays less than 0.4 cm because of preceding misalignments, it is reasonable to set 0.4 cm as the y displacement tolerance.

There is no way to fix the x- and y-rotational tolerances because errors measured in degrees cause negligible shifts in the central trajectory. These tolerances are arbitrarily fixed at 20 mr.

Tolerances on Bending Magnets B_1

Axis	Translation	Rotation
x	[1. cm]	[20. mr]
y	0.4 cm	[20. mr]
z	0.4 cm	0.11 mr (3.3 with steering)

F. Symmetry Quadrupole Q_2

Misalignment Type	Misalignment Axis	Uncertainty Axis	Uncertainty Magnitude at Location			
			D3	B2	D4	Target
Disp	x	x	.14 cm/mm	.24 cm/mm	.28 cm/mm	.00 cm/mm
Disp	y	y	.15	.24	.02	.00
Rotn	x	y	.003 cm/mr	.004 cm/mr	.013 cm/mr	.00 cm/mr
Rotn	y	x	.001	.000	.007	.001

The main concern in setting alignment tolerances on the symmetry quad is that alignment errors should not cause the beam to hit any of the downstream magnet apertures. In the vertical plane this means holding the displacement at B2 to less than 0.46 cm. This fixes the y-displacement tolerance at $0.46/3 \times 0.24 = 0.62$ mm = 25 mils. The extra factor of 3 helps relax the y-displacement tolerance on Q_1. Steering the beam would essentially remove the tolerance on Q_2.

In the horizontal plane, the bending magnets have an aperture of ±8.25 cm but the quads following the bend have a ±3.65-cm bore. As the horizontal beam size at the exit of Q_3 is 1.8 cm, the central trajectory should not wander more than 1.2 cm. This fixes the x-displacement tolerance at $1.2/0.24 = 5$ mm.

Rotational tolerances have arbitrarily been set at 1 mr.

The symmetry quad may be shifted ±5 cm in the z direction without appreciably disturbing the achromaticity of the system.

Tolerances on Symmetry Quad, Q_2

Axis	Translation	Rotation
x	0.5 cm	[1 mr]
y	25. mils	[1 mr]
z	5. cm	[1 mr]

The main detrimental effect of the symmetry quad is that it amplifies errors in the vertical plane caused by misalignments in the front half of the system.

G. Bending Magnets B_2

Misalignment Type	Misalignment Axis	Axis	Uncertainty Magnitude at Location		
			B2	D4	Target
Disp	x	x	.000 cm/mm	.000 cm/mm	.000 cm/mm
Disp	y	y	.002	.040	.001
Disp	z	x	.010	.023	.007
Rotn	x	y	.000 cm/mr	.002 cm/mr	.000 cm/mr
Rotn	y	x	.000	.000	.000
Rotn	z	y	.11	2.22	.06

The x-displacement, y-displacement, x-rotation, and y-rotation tolerances are each fixed by the same arguments as those given for the corresponding tolerances on B_1. The z-displacement tolerance can no longer be fixed by considering resolution or apertures, and is set arbitrarily at one centimeter. The z-rotation tolerance can be set by requiring that the beam not wander off the reference axis by more than 1.5 centimeters in the vicinity of Q_4. This gives a tolerance of 1.5/2.22 = 0.7 mr. If a magnet system is inserted between Q_3 and Q_4, then these tolerances as well as those on Q_3 will have to be reviewed.

Tolerances on Bending Magnets B_2

Axis	Translation	Rotation
x	[1. cm]	[20. mr]
y	0.3 cm	[20. mr]
z	[1. cm]	0.7 mr (more with steering)

H. Quadrupole Doublet Q_3

Misalignment Type	Misalignment Axis	Uncertainty Axis	Uncertainty Magnitude at Location: D_4	Uncertainty Magnitude at Location: Target
Disp	x	x	2.07 cm/mm	0.40 cm/mm
Disp	y	y	2.92 cm/mm	0.09 cm/mm

The table above was derived under the assumption that both magnets in the doublet were aligned independently. The alignment derivatives for the doublet mounted on a frame are given in the Appendix.

The only criteria for setting tolerances on the alignment of Q_3 is that the beam get through the quadrupole doublet Q_4 or whatever phase-matching device is located at the end of the arbitrary drift space D_4. As an example, D_4 was set at 200 meters and Q_4 was taken to be a quadrupole doublet with a 4-centimeter bore radius. The beam radius is 1.5 cm at the entrance to Q_4, which means that the central trajectory should not wander more than about 1.5 cm from the desired location. From this requirement the tolerances are found to be:

x-displacement = 1.5/2.07 = 0.7 mm = 29 mils

y-displacement = 1.5/2.92 = 0.5 mm = 21 mils

The z-displacement tolerance and the rotation tolerances were fixed more or less arbitrarily. Since there may be steering in this region, these tolerances are probably not too meaningful.

Tolerances on Doublet Q_3

Axis	Translation	Rotation
x	29. mils	[1 mr]
y	21. mils	[1 mr]
z	[5. cm]	[1 mr]

I. Combined Errors

Table VII gives a complete set of tolerances for all of the magnets in system A. As a final test of these tolerances, all the magnets in system A were given alignment uncertainties in accordance with the values in this table, and the cumulative effect on the beam was traced through the system. The beam stays within all the magnet apertures as required and the net displacement of the beam at the slit is 0.13 cm, as required.

If at any time during the operation of the machine the alignment of the switchyard is in question, and if the remote measuring devices can give values for the various misalignments, these values can be processed by TRANSPORT and their effect on the beam evaluated.

J. Tolerances

The feasibility of the tolerances given in Table VII (and in Table XIII for System B) are summarized below.*

a. Rotation

A tolerance of 1 milliradian (mr) is equivalent to about 200 seconds of arc, or to a slope of 0.001. Thus, over a 1-meter span, a relative height difference of 1 mm, or 40 mils, would be 1 mr. For an alignment tolerance of 0.1 mr, a relative height difference of 4 mils over a 1-meter span would have to be held. It is felt that movement due to environmental effects, such as settlement, temperature, etc., will be reasonably uniform to allow this latter tolerance to be held.

b. Translation

It is felt that translation along the beam (z) axis of 1 mm (40 mils) can be readily held. Translations from the ideal beam centerlines can be held to a few mils or about 0.1 mm on the vertical plane where necessary. In the horizontal plane, translations from the ideal central trajectory can probably be held to 5 mils probable error at the critical Q_1 doublet because of its proximity to the optical alignment tube of the accelerator itself. The probable error of the positions of the elements will increase as the A and the B beams diverge from the central beam. The tolerance achievable at the second doublet is on the order of 10 mils.

*J. Voss, Private Communication.

TABLE VII

Alignment Tolerances – System A

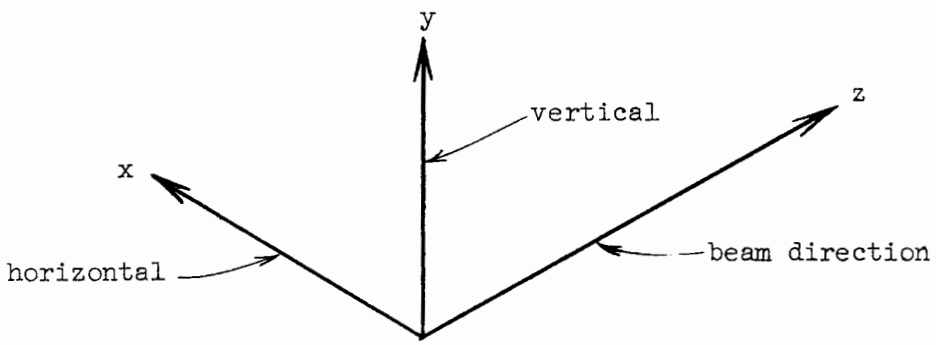

Magnet	Axis	Translation (cm)	Rotation About Axis (mr)
Switching	x	[1]	[20]
Magnet	y	1.	[20]
P	z	[1]	1.5
Quadrupole	x	0.0254	[1]
Doublet	y	.0051 (more w/s)*	[1]
Q_1	z	4.	[1]
Bending	x	[1]	[20]
Magnets	y	0.75	[20]
B_1	z	.4	0.11 (3.3 w/s)
Symmetry	x	0.5 (more w/s)	[1]
Quad	y	0.0254 (more w/s)	[1]
Q_2	z	5.0	[1]
Bending	x	[1]	[20]
Magnets	y	0.75	[20]
B_2	z	0.4	0.7 (more w/s)
Quadrupole	x	.074	[1]
Doublet	y	.053	[1]
Q_3	z	[5]	[1]

*w/s stands for "with steering."

VII. SYSTEM B

A. Design Criteria

Energy

The design momentum was fixed at 25 GeV/c. However, the system was planned so that operation at 40 GeV/c would be possible with minor modifications.

Beam Size

Same as system A--0.3 cm.

Beam Divergence

Same as system A--10^{-4} radians.

Momentum Spread

The design momentum spread is ±3%.

Resolution

The transport system must be capable of resolving ±0.1% in momentum independent of the operation of the accelerator and of the performance of the pulsed switching magnet. Long-term repeatability must be ±0.02%.

Achromaticity

The system must be achromatic.

Isochronism

After passing through the system, the longitudinal extent of the bunch must not exceed ±20° in rf phase (at 2856 Mc/sec) for p/p = ±3%.

B. Qualitative Description of System B

The design philosophy for system B is identical to that for system A. The total angle of bend is 12.5°, derived from two 6° bends and a 0.5° deflection by the pulsed switching magnet. The smaller total angle of bend was necessitated by the larger momentum spread (±3%) and the desire to use magnets of the same design in both systems. Two 3-meter magnets, each bending 3°, are used to obtain the 6° bend. (The two magnets in each set are separated by 6 meters to allow the future insertion of a

third magnet for possible expansion into Stage II accelerator operation at 40 GeV/c. Each magnet then will bend only 2°.)

The polarity of the doublet Q_1 in system B was chosen to be (+-), which is the reverse of system A. While the (-+) configuration would give a better ultimate resolution (by a factor of 2), the (+-) arrangement yields more than enough to meet the design criteria and, at the same time, relaxes the horizontal aperture requirement in Q_1, which is more severe than in system A due to the dispersing effect of the pulsed magnet upon the larger momentum spread.

C. Results of First-Order Design Calculations

The results of the TRANSPORT run are given in Fig. 10 and in Tables VIII, IX, and X. Figure 10 displays the beam envelope of the system. It appears at first that the beam exceeds the aperture of the symmetry quadrupole, but is must be kept in mind that while the bore radius is only 9.3 cm, the useful horizontal half-aperture is more nearly 18 cm because of the design adopted for the quadrupoles. From the envelope trace it is possible to obtain the apertures necessary to pass the specified phase space. They are:

	Horizontal	Vertical
Doublets	2.33 cm	1.31 cm
Symmetry Quad	9.44	0.1
Bending Magnets	2.81	1.31

The magnets in system B will be identical to those used for system A. The magnet apertures are given in Table IV.

Table VIII gives the magnet parameters and drift distances for the system at 25 GeV/c. Table IX gives the same information for Stage II operation at 40 GeV/c. Table X contains the data needed to draw a floor layout of the 25 GeV/c system.

The minimum resolution for system B is

$$\delta_{min} = \frac{0.708 \times 0.3}{3.15} = 0.067\%$$

The slit width which passes a given momentum interval is given by

$$w = \pm 3.15\ \delta \text{ cm}$$

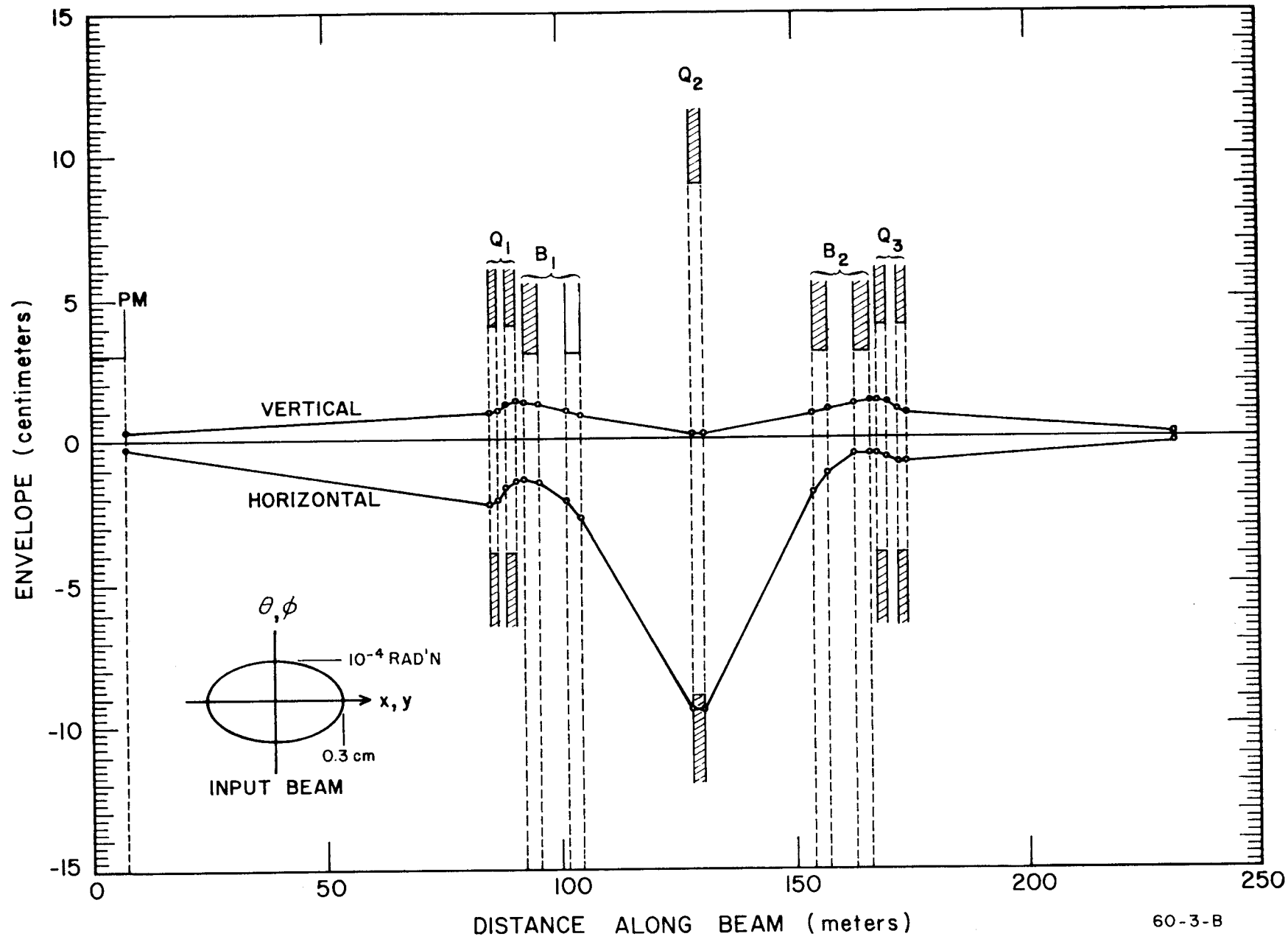
15
10
5
0
-5
-10
-15
ENVELOPE (centimeters)
PM
Q_1
B_1
Q_2
B_2
Q_3
VERTICAL
HORIZONTAL
θ, ϕ
10^{-4} RAD'N
x, y
0.3 cm
INPUT BEAM
0
50
100
150
200
250
DISTANCE ALONG BEAM (meters)
60-3-B

FIGURE 10

TABLE VIII

SYSTEM B PARAMETERS (25 GeV/c)

Element Type	Magnetic Length (meters)	Field at Pole (kG)	Bore (2a) (cm)	Pole Rotation β_1 (deg)	β_2
Bend*	7	1.04 (1.774)		0	0.5
Drift	-18.5				
Quad	2.	1.735	8.		
Drift	2.				
Quad	2.	-1.804	8.		
Drift	1.5				
Bend (3°)	3	14.55		1.5°	1.5°
Drift	6				
Bend (3°)	3	14.55		1.5°	1.5°
Drift	23.94				
Quad	2.	2.410	18.6†		
Drift	24.06				
Bend (3°)	3.	14.55		1.5°	1.5°
Drift	6.				
Bend (3°)	3.	14.55		1.5°	1.5°
Drift	1.5				
Quad	2.	-1.918	8.		
Drift	2.				
Quad	2.	1.867	8.		
Drift	57.				

*The pulsed bending magnet actually consists of five magnets, each having a magnetic length of 0.82 meters. They are mounted on a frame, the whole configuration being 7 meters long. The field given in parentheses corresponds to 4.1 meters of magnet, not 7.

†See remark following Table IV, p. 17.

TABLE IX

PHASE II SYSTEM B PARAMETERS (40 GeV/c)

Element Type	Length (meters)	Field at Pole (Kg)	Bore (2a) (cm)	Pole Rotation β_1 (deg)	β_2
Bend	7.	1.664		0.	0.5
Drift	78.5				
Quad	2.	-2.794	8.		
Drift	2.				
Quad	2.	2.937	8.		
Drift	1.5				
Bend	3.	15.54		1.	1.
Drift	1.5				
Bend	3.	15.54		1.	1.
Drift	1.5				
Bend	3.	15.54		1.	1.
Drift	23.69				
Quad	2.	3.563	18.6		
Drift	24.01				
Bend	3.	15.54		1.	1.
Drift	1.5				
Bend	3.	15.54		1.	1.
Drift	1.5				
Bend	3.	15.54		1.	1.
Drift	1.5				
Quad	2.	-2.192	8.		
Drift	2.				
Quad	2.	2.154	8.		
Drift	Variable				

TABLE X

SYSTEM B LAYOUT

	Element Type	Effective Length (meters)	Bend Angle (deg)	Total Length Along CT (meters)	Total Bend Angle (deg)	Coordinates of Vertex of Magnet X (meters)	X (feet)	Y (meters)	Y (feet)	Z (meters)	Z (feet)
P	BEND	7.00	.50	7.00	.50	.00	.0	-.02	-.1	3.50	11.5
	DRIFT	78.50		85.50	.50						
Q_1	QUAD	2.00		87.50	.50	.72	2.4	-.39	-1.3	86.50	283.8
	DRIFT	2.00		89.50	.50						
	QUAD	2.00		91.50	.50	.76	2.5	-.41	-1.4	90.50	296.9
	DRIFT	1.50		93.00	.50						
B_1	BEND	3.00	3.00	96.00	3.50	.79	2.6	-.43	-1.4	94.50	310.0
	DRIFT	3.00		99.00	3.50						
	DRIFT	3.00		102.00	3.50						
	BEND	3.00	3.00	105.00	6.50	1.34	4.4	-.46	-1.5	103.48	339.5
	DRIFT	23.94		128.94	6.50						
Q_2	QUAD	2.00		130.94	6.50	4.33	14.2	-.52	-1.7	129.75	425.7
	DRIFT	24.06		155.00	6.50						
B_2	BEND	3.00	3.00	158.00	9.50	7.34	24.1	-.58	-1.9	156.14	512.3
	DRIFT	3.00		161.00	9.50						
	DRIFT	3.00		164.00	9.50						
	BEND	3.00	3.00	167.00	12.50	8.82	28.9	-.59	-1.9	165.02	541.4
	DRIFT	1.50		168.50	12.50						
Q_3	QUAD	2.00		170.50	12.50	9.69	31.8	-.59	-1.9	168.92	554.2
	DRIFT	2.00		172.50	12.50						
	QUAD	2.00		174.50	12.50	10.55	34.6	-.59	-1.9	172.83	567.0
	DRIFT	57.00		231.50	12.50						

64-2A

where δ is in percent. For $\delta = 0.1\%$

$$w = \pm 0.315 \text{ cm}$$

The longitudinal extent of an electron bunch grows 10° in rf phase (0.3 cm) in passing through system B. This loss in isochronism is due entirely to the $\pm 3\%$ momentum spread via the $(z|\delta_o)$ matrix element.

The last doublet of system B is adjusted to produce a double waist 57 meters downstream. This adjustment is orthogonal to the rest of system B.

The tracking requirements for system B are essentially the same as those for system A; that is, the current in the bending magnets must be controlled and resettable to one part in 10,000, while the fluctuations in $\Delta B/B$ of the magnets can be as high as 3 to 4 parts per 10,000.

The effect of the earth's magnetic field on system B is the same as on system A. For phase II operation at 40 GeV/c, the deflection of the central trajectory will only be 0.06 cm at the slit, with corresponding improvement in the vertical deflection inside B_2.

D. Second Order

The effects of second-order aberrations on system B are essentially the same as those for system A. The main difference is that the reversed polarity of the doublet Q_1 reduces the sensitivity of the aberrations to magnet imperfections. If the doublet converges horizontally first then particles of a given momentum stay closer to the central trajectory and pass through a more homogenous region of the magnets. This difference is important because it offsets effects of the larger momentum acceptance of system B. The values $\frac{\Delta x_1}{w}$ and $\frac{\Delta x_2}{w}$, discussed in Section V, are tabulated for system B below. Note that the first-order magnification is .70 here, more than twice that of A.

	Initial beam divergence is 10^{-4} radians			Initial beam divergence is 10^{-5} radians		
	$\frac{\Delta x_1}{w}$	$\frac{\Delta x_2}{w}$	at $\delta = 1\%$	$\frac{\Delta x_1}{w}$	$\frac{\Delta x_2}{w}$	at $\delta = 1\%$
$\epsilon_1 = 0$	~0	.16		~0	.05	
$\epsilon_1 = 2 \times 10^{-5}$	.062	.18		.005	.06	
$\epsilon_2 = 10^{-4}$	.29	.25		.033	.08	

The table below gives estimates for the target spot size

	first order	$\epsilon = 0$	$\epsilon_1 = 2 \times 10^{-5}$	$\epsilon_1 = 10^{-4}$
est. x spot size	.20	.27	.29	.40
est. y spot size	.19	.20	.32	.39
mean x displacement	0	-.07	-.09	-.19
mean y displacement	0	0	0	0

The difference in path length at the target between the centroid of the bunch and the reference particle is -.1 cm. This is larger than in A solely because of the larger allowable momentum deviations (3%) of the particles in the bunch.

E. Alignment Tolerances

The method for studying the effects of magnet misalignments in system B was the same as that used for system A. The result of each error was evaluated by TRANSPORT and a table of derivatives was prepared. Using the table together with the magnet apertures and system resolution requirements given below, it was possible to establish tolerances on the alignment of the system.

1. Alignment Criteria

The only magnet aperture that gives rise to severe alignment tolerances is that of the second bending magnet in B_2. As in system A, the usable aperture is only ±2.37 cm and the beam is ±1.31 cm at that point. the requirement for a 0.5-cm safety margin leaves only ±2.37 - 1.31 - 0.5 = 0.5 cm for errors due to alignment. This is reduced further by a factor of $\sqrt{2}$ because there are two major errors contributing to this displacement, and it then becomes 0.36 cm.

The resolution of system B is ±0.10% through a ±0.315 cm slit. To hold the same ±0.02% repeatability tolerance specified for system A, the horizontal displacement at the slit due to errors can be no more than $0.315 \times (0.02/0.10) = 0.063$ cm. Thus the 0.02% tolerance makes alignment twice as difficult for system B because the dispersion is half that of system A.

2. Pulsed Magnet

Because the same magnet services both the A and B systems, it is not necessary to repeat the tolerances given in Sec. VI for the pulsed magnet. Note that the tighter vertical displacement allowance of 0.36 cm must replace the number 0.46 cm in the calculation of the z rotation tolerance.

3. Quadrupole Doublet Q_1

The two quadrupoles making up the doublet were assumed to be independently mounted. Both singlets were given the same uncertainty in placement and the results are recorded in Table XI. The x-displacement tolerance is fixed by the resolution tolerance at 0.063/0.018 = 3.5 mils. The y-displacement tolerance is fixed by the vertical gap at B2 to be 0.36/0.054 = 7.0 mils. The rotational and z-displacement tolerances are fixed arbitrarily at 1 mr and 5 cm, respectively.

Tolerances on Doublet Q_1

Axis	Translation	Rotation
x	3.5 mils	[1 mr]
y	7.0 mils	[1 mr]
z	[5. cm]	[1 mr]

4. Bending Magnets, B_1

Table XII was prepared by giving both bending magnets comprising B_1 the alignment uncertainty associated with a particular line in the table.

The z-displacement tolerance was fixed by resolution considerations to be 0.063/3 × 0.007 = 3 mm. (The added factor of 3 was inserted to relax the tolerance on Q_1.) The y-displacement tolerance was set at 0.5 cm so that the (possibly misaligned) beam does not hit the pole of the magnet itself. The z-rotation tolerance was set at 0.36/1.09 = 0.34 mr to keep the beam from striking the second set of bending magnets. The other tolerances are arbitrary.

Tolerances on Bending Magnets B_1

Axis	Translation	Rotation
x	[1. cm]	[20. mr]
y	0.5 cm	[20. mr]
z	0.3 cm	0.34 mr

TABLE XI

ALIGNMENT DERIVATIVES FOR QUADRUPOLE DOUBLET Q_1

Misalignment Type	Misalignment Axis	Uncertainty Axis	Uncertainty Magnitude at Location			
			Slit	D3	B2	Target
Disp	x	x	.018 cm/mil	.001 cm/mil	.009 cm/mil	.019 cm/mil
Disp	y	y	.014	.040	.054	.024
Rotn	x	y	.008 cm/mr	.026 cm/mr	.037 cm/mr	.013 cm/mr
Rotn	y	x	.014	.001	.010	.014

TABLE XII

ALIGNMENT DERIVATIVES FOR BENDING MAGNETS B_1

Misalignment Type	Misalignment Axis	Uncertainty Axis	Uncertainty Magnitude at Location			
			Slit	D3	B2	Target
Disp	x	x	.000 cm/mm	.000 cm/mm	.000 cm/mm	.000 cm/mm
Disp	y	y	.004	.014	.019	.008
Disp	z	x	.007	.004	.010	.008
Rotn	x	y	.000 cm/mr	.000 cm/mr	.001 cm/mr	.000 cm/mr
Rotn	y	x	.000	.000	.000	.000
Rotn	z	y	.26	.80	1.09	.45

5. Symmetry Quadrupole Q_2

Misalignment Type	Axis	Axis	Uncertainty Magnitude at Location		
			D3	B2	Target
Disp	x	x	0.16 cm/mm	0.24 cm/mm	0.04 cm/mm
Disp	y	y	0.16	0.25	0.02
Rotn	x	y	0.004 cm/mr	0.005 cm/mr	0.004 cm/mr
Rotn	y	x	0.000	0.000	0.002

To keep the beam from striking the poles of B_2, the y-displacement tolerance is fixed at $0.36/3 \times 0.25 = 0.48$ mm, or 20 mils. (The added factor of 3 was inserted to relax the tolerance on Q_1.) The x-displacement tolerance is fixed at $1.5/0.24 = 6$ mm to keep the beam away from the horizontal aperture of the doublet Q_3. The symmetry quad may be shifted ±5 cm in the z-direction without appreciably disturbing the achromaticity of the system. The rotational tolerances are more or less arbitrary.

Tolerances on Symmetry Quad Q_2

Axis	Translation	Rotation
x	0.6 cm	[1 mr]
y	20. mils	[1 mr]
z	5. cm	[1 mr]

6. Bending Magnets B_2

Misalignment Type	Axis	Axis	Uncertainty Magnitude at Location	
Disp	x	x	0.000 cm/mm	0.000 cm/mm
Disp	y	y	0.001	0.009
Disp	z	x	0.005	0.004
Rotn	x	y	0.000 cm/mr	0.000
Rotn	y	x	0.000	0.000
Rotn	z	y	0.069	0.500

The y-displacement tolerance is fixed at 0.1 cm to keep the beam (possibly displaced because of misalignments of preceding elements) from hitting the magnet proper. The z-rotation tolerance is fixed at 1. mr to keep the beam spot from wandering more than 0.5 cm at the target. The other tolerances are more or less arbitrary.

Tolerances on Bending Magnets B_2

Axis	Translation	Rotation
x	[1. cm]	[20. mr]
y	0.1 cm	[20. mr]
z	[1. cm]	1. mr

7. Quadrupole Doublet Q_3

Each quadrupole was treated as an independently mounted unit and the same uncertainty in placement was applied to each member.

Misalignment Type	Misalignment Axis	Uncertainty Axis	Uncertainty Magnitude at Location
			Target
Disp	x	x	0.74 cm/mm
Disp	y	y	1.15
Rotn	x	y	0.014 cm/mr
Rotn	y	x	0.019

The only boundary condition that can be invoked to fix the tolerances on Q_3 are that the beam cannot wander more than about 0.5 cm from the specified target location. This leads to the following tolerances.

x-dixplacement = 0.5/0.74 = 0.6 mm = 24 mils

y-displacement = 0.5/1.15 = 0.44 mm = 18 mils

The other tolerances are more or less arbitrarily fixed.

Tolerances on Doublet Q_3

Axis	Translation	Rotation
x	24. mils	[1 mr]
y	18. mils	[1 mr]
z	[5. cm]	[1 mr]

F. Combined Errors

Table XIII gives a complete set of tolerances for all the magnets in system B. As a final test of these tolerances, all the magnets in system B were given alignment uncertainties in accordance with the values in this table and the cumulative effect on the beam was traced through the system. The beam stays within all magnet apertures as required, and the net displacement of the beam at the slit is less than the 0.63 mm specified.

TABLE XIII

ALIGNMENT TOLERANCES FOR SYSTEM B

Magnet	Axis	Translation (cm)	Rotation About Axis (mr)
Quadrupole	x	.0089	[1]
Singlets	y	.0089	[1]
Q_1	z	[5]	[1]
Bending	x	[1]	[20]
Magnets	y	1.	[20]
B_1	z	0.3	0.17
Symmetry	x	0.6	[1]
Quadrupole	y	0.025	[1]
Q_2	z	5.	[1]
Bending	x	[1]	[20]
Magnets	y	1.	[20]
B_2	z	[1]	1.
Quadrupole	x	.061	[1]
Singlets	y	.048	[1]
Q_3	z	[5]	[1]

REFERENCES

1. S. Penner, "Electron beam deflection systems for the Monster," M Report No. 200-13, Stanford Linear Accelerator Center, Stanford University, Stanford, California (Summer 1960).
2. C. Moore, S. Howry, and H. Butler, "TRANSPORT--A computer program for designing beam transport systems," Internal Report, Stanford Linear Accelerator Center, Stanford University. Stanford, California (March 1963).
3. A. Odian, "The weak (parasitic) γ beam," Internal Memorandum, Stanford Linear Accelerator Center, Stanford University, Stanford, California (December 1963).
4. S. Howry, "Second order aberration coefficients of a quadrupole," Internal Memorandum, Stanford Linear Accelerator Center, Stanford University, Stanford, California (August 1962).
5. R. Belbeoch, P. Bounin, and K. Brown, "The first- and second-order magnetic optics matrix equations for the midplane of uniform-field wedge magnets," Rev. Sci. Instr. 35, 4, 481 (April 1964).
6. K. Brown, "The first- and second-order aberration coefficients of wedge magnets," Internal Memorandum, Stanford Linear Accelerator Center, Stanford University, Stanford, California (February 1963).
7. S. Howry, "Off-midplane second order coefficients for an ideal bending magnet," Internal Memorandum, Stanford Linear Accelerator Center, Stanford University, Stanford, California (December 1963).
8. R. Helm, "First and second order beam optics of a curved, inclined magnetic field boundary in the impulse approximation," SLAC Report No. 24, Stanford Linear Accelerator Center, Stanford University, Stanford, California (November 1963).

APPENDIX

For the sake of completeness, the alignment tolerances for doublets Q_1 and Q_3, each aligned as a unit on a rigid frame, are presented here. The rotational tolerances on Q_1 are very stringent because the principal planes of the lens are located far outside the body of the doublet; thus a small rotation of the frame leads to a large movement of the principal planes. This fact suggests that Q_1 be replaced by a triplet, because the principal planes of a triplet are usually located near the center of the lens. This possibility was studied, and the results are recorded here. It was found that the collinearity tolerances on the individual elements of the triplet are too stringent to be maintained. Therefore, it was decided that independent alignment of each magnet in Q_1 and Q_3 was the best method.

I. QUADRUPOLE DOUBLET Q_1

Table A-I gives the alignment derivatives for the quadrupole doublet Q_1. In preparing this table, it was assumed that the two quadrupoles which make up the doublet were perfectly aligned on a rigid frame. The frame was then misaligned about its center.

The requirement for reproducible resolution at the slit fixes tolerances on those alignment errors which lead to radial displacements of the beam at the slit. This displacement should be held to $0.13/\sqrt{2} = 0.1$ cm because now there are two major contributions to the error. The x-displacement tolerance is thus fixed at $0.10/0.128 = 0.8$ mm, and the y-rotation must not exceed $0.10/1.43 = 0.07$ mr. These tolerances are also sufficient to assure that the beam will stay within the apertures of the magnets which follow the slit.

The y-displacement tolerance is chosen to keep the beam off the poles of the second set of bending magnets. On page 33, the maximum vertical displacement of the beam was set at 0.46 cm. This yields a tolerance of $0.46/0.66 = 0.70$ mm = 28 mils. If the beam is to be steered, then this tolerance can be relaxed, and only the vertical aperture of the spectrum analyzer need be considered in this case. The necessity of keeping the

TABLE A-I

QUADRUPOLE DOUBLET Q_1

Misalignment Type	Misalignment Axis	Uncertainty Axis	Uncertainty Magnitude at Location					
			B1	Slit	D3	B2	D4	Target
Disp	x	x	0.058 cm/mm	0.128 cm/mm	0.040 cm/mm	0.020 cm/mm	0.468 cm/mm	0.080 cm/mm
Disp	y	y	0.11	0.17	0.47	0.66	1.10	0.00
Rotn	x	y	1.3 cm/mr	2.3 cm/mr	6.6 cm/mr	9.2 cm/mr	14.7 cm/mr	0.00 cm/mr
Rotn	y	x	0.90	1.43	0.13	0.77	5.93	0.90

central trajectory within 1.25 cm of the center of the analyzer sets a tolerance of 1.25/0.17 = 7 mm.

The x-rotation tolerance is fixed by aperture considerations. Without steering the tolerance is 0.46/9.2 = 0.05 mr; with steering it is 1.25/2.3 = 0.55 mr.

A four-centimeter displacement of the doublet along the z-axis causes a 20% decrease in resolution or, conversely, a 20% increase in the momentum spread passing a fixed width slit. A rotation of 20 mr about the z-axis does not markedly affect the beam optics.

Tolerances on Doublet Q_1

Axis	Translation	Rotation
x	0.8 mm	0.05 mr (0.55 mr ws)
y	28.0 mils (7.0 mm ws)	0.07 mr
z	4.0 cm	[20 mr]

The tolerances given in this table are based on the model of a perfectly aligned doublet mounted on a rigid frame. Associated with this model are tolerances on the alignment of each element of the doublet on the frame. Tolerances on four of the degrees of freedom are trivial -- 1 cm in the z direction and 20 mr on each rotational degree of freedom, provided the rotation is performed about the physical center of the magnet. The non-collinearity tolerance (the displacement of the magnetic axis of one quadrupole from the ideal magnetic axis of the doublet) in the x direction is 0.09 mm = 3.6 mils, and is 0.3 mm = 12 mils in the y direction.

Inter-Element Tolerances on Doublet Q_1

Axis	Translation	Rotation
x	3.6 mils	[20 mr]
y	12.0 mils	[20]
z	1.0 cm	[20]

The reason Q_1 is so sensitive to alignment errors is that its principal planes are far outside the body of the lens. Figure A-1 shows the location of the principal planes. A small rotation of Q_1 about its center causes a large displacement of the principal planes and hence a large effect on the beam.

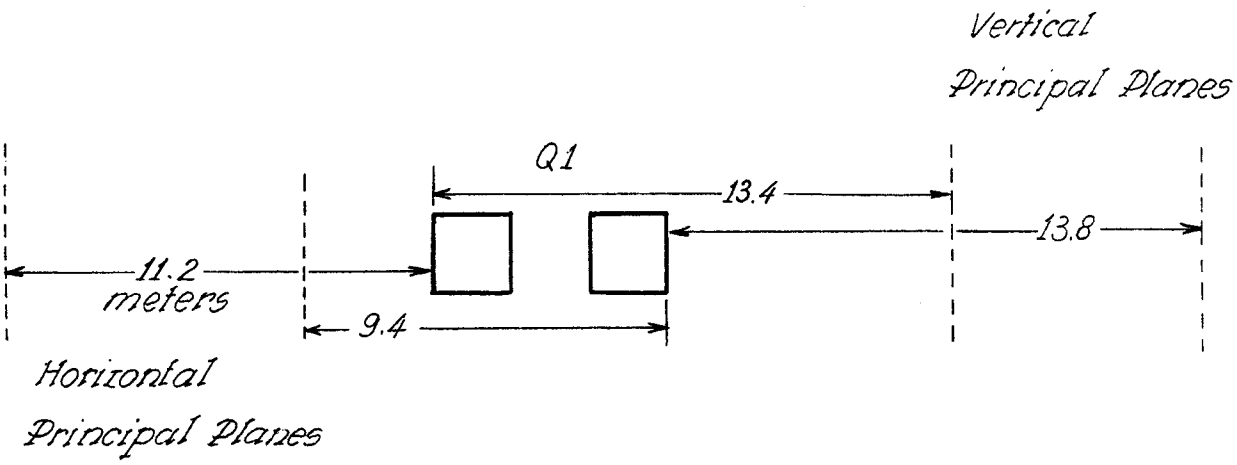

Figure A-1

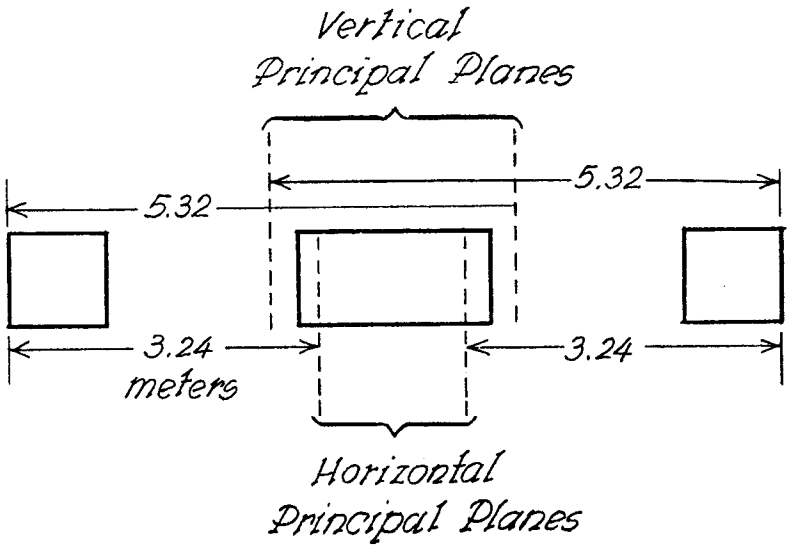

Figure A-2

The way to circumvent this difficulty is to substitute a triplet for the doublet. Figure A-2 shows the location of the principal planes of a symmetric triplet with gradients that give double focusing at the slit, just as the doublet did.

II. QUADRUPOLE TRIPLET Q_1

Table A-II gives the alignment derivatives for the quadrupole triplet Q_1. In the preparation of this table, the three quadrupoles which make up the triplet were assumed to be perfectly aligned on a rigid frame. The frame was then misaligned about its center.

The x-displacement tolerance is fixed by the resolution criteria to be 0.13/0.15 = 0.9 mm. The y-displacement tolerance is fixed by the aperture requirement at B2 to be 0.46/0.58 = 0.79 mm = 32 mils; if steering is contemplated, the tolerance can be relaxed to 1.25/0.15 = 8 mm and still keep the beam within the aperture of the spectrum analyzer at the slit.

The effect of a rotation of the triplet about its center is so small that no reasonable tolerance can be given. The two rotation tolerances are arbitrarily set at 20 mr. The tolerances along and about the z-axis are the same as for the doublet.

Tolerances on Triplet Q_1

Axis	Translation	Rotation
x	0.9 mm	[20 mr]
y	32.0 mils (8.0 mm ws)	[20]
z	4.0 cm	[20]

The use of a triplet for Q_1 as opposed to a doublet makes an enormous improvement in the rotation tolerances about the x and y axes. However, there is a price to be paid for such benefits. The gradients of the triplet are 55% higher for the same length of iron. The frame for the particular triplet configuration chosen here is 8 meters vs 6 for the doublet. Finally, the non-collinearity tolerances for the elements of the triplet are quite severe -- on the order of 0.2 mil. This essentially removes the triplet from contention.

TABLE A-II

QUADRUPOLE TRIPLET Q_1

Misalignment Type	Misalignment Axis	Uncertainty Axis	Uncertainty Magnitude at Location					
			B1	Slit	D3	B2	D4	Target
Disp	x	x	0.09 cm/mm	0.15 cm/mm	0.01 cm/mm	0.07 cm/mm	0.60 cm/mm	0.09 cm/mm
Disp	y	y	0.09	0.15	0.42	0.58	0.94	0.00
Rotn	x	y	0.014 cm/mr	0.005 cm/mr	0.001 cm/mr	0.001 cm/mr	0.034 cm/mr	0.001 cm/mr
Rotn	y	x	0.008	0.003	0.008	0.016	0.031	0.002

III. QUADRUPOLE DOUBLET Q_3

The alignment derivatives for the quadrupole doublet Q_3 are given below.

Misalignment Type	Misalignment Axis	Uncertainty Axis	Uncertainty Magnitude at Location: D4	Uncertainty Magnitude at Location: Target
Disp.	x	x	0.52 cm/mm	0.066 cm/mm
Disp.	y	y	0.70	0.02
Rotn.	x	y	8.3 cm/mr	0.20 cm/mr
Rotn.	y	x	5.9	1.1

The criteria used in Section VI to set the tolerances on the individual elements of Q_3 can be applied here. They lead to the following tolerances on the frame-mounted doublet.

x-displacement = 1.5/0.52 = 3 mm
y-displacement = 1.5/0.70 = 2 mm
x-rotation = 1.5/2.3 = 0.18 mr
y-rotation = 1.5/5.9 = 0.25 mr

The z-displacement and rotation tolerances are set arbitrarily at 5 cm and 20 mr, respectively.

Tolerances on Doublet Q_3

Axis	Translation	Rotation
x	3.0 mm	0.18 mr
y	2.0 mm	0.25
z	[5 cm]	[20]

LEGAL NOTICE